Integrable and Conformal Boundary Conditions for $\hat{s\ell}(2)$ A–D–E Lattice Models and Unitary Minimal Conformal Field Theories

Roger E. Behrend

C. N. Yang Institute for Theoretical Physics

State University of New York

Stony Brook, NY 11794-3840, USA

Roger.Behrend@sunysb.edu

Paul A. Pearce

Department of Mathematics and Statistics

University of Melbourne

Parkville, Victoria 3052, Australia

P.Pearce@ms.unimelb.edu.au

Abstract

Integrable boundary conditions are constructed for the critical A–D–E lattice models of statistical mechanics. In particular, using techniques associated with the Temperley-Lieb algebra and fusion, a set of explicit boundary Boltzmann weights which satisfies the boundary Yang-Baxter equation is obtained for each boundary condition. When appropriately specialised, these boundary weights, each of which depends on three spins, decompose into more natural two-spin edge weights. The specialised boundary conditions are also naturally in one-to-one correspondence with the conformal boundary conditions of $\hat{s\ell}(2)$ unitary minimal conformal field theories. Supported by this and further evidence, we conclude that, in the continuum scaling limit, the integrable boundary conditions provide realisations of the complete set of conformal boundary conditions in the corresponding field theories.

1. Introduction and Overview

The notion of conformal boundary conditions in conformal field theories, in the sense introduced in [1], and the notion of integrable boundary conditions in integrable lattice models, in the sense introduced in [2], are both well developed. It is also well known that conformal field theories can be identified with the continuum scaling limit of certain critical integrable lattice models of statistical mechanics. A natural question to address, therefore, is whether similar associations can be made between the corresponding boundary conditions. We shall demonstrate here that indeed they can. In so doing, not only is the existence of deep connections between conformal and integrable boundary conditions established, but a means is also provided for gaining insights, generally not available within conformal field theory alone, into the physical nature of conformal boundary conditions.

That there should be a relationship between such integrable and conformal boundary conditions is not immediately apparent and, accordingly, the correspondence is somewhat subtle. It is known that nonintegrable boundary conditions can be identified with certain conformal boundary conditions and, conversely, we expect that integrable boundary conditions will only lead to conformal boundary conditions upon suitable specialisation. Nevertheless, we shall explicitly show for all of the $\hat{s\ell}(2)$ cases considered here that an integrable boundary condition can, after such specialisation, be naturally associated with every conformal boundary condition. Furthermore, the generality of the approach used here suggests that it is possible to construct an integrable boundary condition corresponding to each allowable conformal boundary condition in any rational conformal field theory which is realisable as the continuum scaling limit of a Yang-Baxter-integrable lattice model.

The basic context for this work is provided by certain general results on boundary conditions. For statistical mechanical lattice models, it is well known from [3] that a model is integrable on a torus by commuting transfer matrix techniques if its Boltzmann weights satisfy the Yang-Baxter equation. A result of [2] then states that such a model is similarly integrable on a cylinder with particular boundary conditions if corresponding boundary Boltzmann weights are used which satisfy a boundary Yang-Baxter equation. A further result, obtained in [4], is that such boundary weights can be constructed using a general procedure involving the process of fusion. In conformal field theory, the main result, obtained in [5, 6, 7] and based on a consistency condition of [1], is that the classification of conformal boundary conditions in rational theories on a cylinder is essentially equivalent to the classification of representations, using matrices with nonnegative integer entries, of the fusion algebra.

In this paper, we consider the critical A–D–E integrable lattice models, as introduced in [8], and the $\hat{s\ell}(2)$ unitary minimal conformal field theories with central charge $c<1$, as first identified in [9, 10] and classified on a torus in [11, 12, 13]. As shown in [14, 15, 16], the continuum scaling limit of these lattice models is described by these field theories. Furthermore, the programme of classifying these theories, and their conformal boundary conditions, on a cylinder was carried out in full in [7], leading to an A–D–E scheme matching that for the torus. Lattice realisations of some of these conformal boundary conditions have been identified and studied in [1, 17, 18, 19, 20, 21, 22, 23, 24, 25, 26, 27], but in most of these cases the lattice boundary conditions are not integrable in the sense of being implemented by boundary weights which satisfy the boundary Yang-Baxter equation.

Here, we use the fusion procedure of [4] to obtain integrable boundary conditions for the A–D–E lattice models and we show that, when appropriately specialised, these can be interpreted as realisations of the complete sets of conformal boundary conditions, as classified in [7], of $\hat{s\ell}(2)$ unitary minimal field theories on a cylinder.

We now provide a detailed overview of the body of this paper. In obtaining the integrable boundary conditions for the A–D–E models, it is convenient to consider a somewhat larger class of integrable lattice models. These models, essentially introduced in [28], are restricted-solid-on-solid interaction-round-a-face models and each is based on a graph $\mathcal{G}$, with the A–D–E models being obtained by taking $\mathcal{G}$ as an A, D or E Dynkin diagram. In such a model, the spin states are the nodes of $\mathcal{G}$, there is an adjacency condition on the states of neighbouring spins given by the edges of $\mathcal{G}$ and the bulk Boltzmann weights are defined in terms of a particular eigenvalue and eigenvector of the adjacency matrix of $\mathcal{G}$. These models are also closely related to the Temperley-Lieb algebra, it being possible to express their bulk weights in terms of matrices of a certain representation of this algebra involving $\mathcal{G}$. The fact that these weights satisfy the Yang-Baxter equation is then a simple consequence of the defining relations of the algebra.

In Section 2, we consider the abstract Temperley-Lieb algebra. The results are thus independent of its representation and apply to the general class of lattice models associated with the Temperley-Lieb algebra, which includes certain vertex models. The main emphasis of Section 2 is on the process of fusion and its use in the construction of boundary operators which correspond to boundary weights. In particular, we list various important properties satisfied by the operators which implement fusion, including projection and push-through properties, and we obtain several results on the properties of the constructed boundary operators, including the facts that they satisfy an operator form of the boundary Yang-Baxter equation and that they can be expressed as a linear combination of fusion operators.

In Section 3, we specialise to representations of the Temperley-Lieb algebra involving graphs and study the corresponding integrable lattice models. We also specialise further to cases where the bulk weights of the model based on graph $\mathcal{G}$ are defined through the Perron-Frobenius eigenvalue and eigenvector of the adjacency matrix of $\mathcal{G}$. For any such model, we then obtain an integrable boundary condition and a related set of boundary weights for each pair (r, a), where r is a fusion level and a is a spin state or node of $\mathcal{G}$. In terms of the procedure of [4], the (r, a) boundary weights are constructed from a fused double block of bulk weights of width $r-1$, with the spin states on the corners of one end of the block fixed to a. These boundary weights each depend on three spins, but we find using results from Section 2 that, upon appropriate specialisation, all of the weights in a set can be simultaneously decomposed into physically more natural two-spin edge weights. We refer to the point at which this occurs as the conformal point, since it is here that we expect correspondence with conformal boundary conditions. While certain integrable boundary weights for some of the models considered here have been obtained in previous studies, specifically [4, 5, 29, 30, 31, 32, 33], this crucial decomposition had not previously been observed. We conclude Section 3 by considering the symmetry properties of a lattice on a cylinder with particular left and right boundary conditions.

In Section 4, we specialise $\mathcal{G}$ to be an A, D or E Dynkin diagram. We obtain completely explicit expressions for the boundary edge weights of the A and D cases and study A_3, A_4, D_4 and E_6 as important examples. We also obtain an important relation through which any A–D–E partition function can be expressed as a sum of certain A partition functions. For all of the A–D–E models, we find that, at the conformal point, the (r,a) and $(g\text{–}r\text{–}1,\bar{a})$ boundary conditions are equivalent, where g is the Coxeter number of $\mathcal{G}$ and $a\mapsto\bar{a}$ is a particular involution of the nodes of $\mathcal{G}$. This implies that these boundary conditions are in one-to-one correspondence with the conformal boundary conditions of the unitary minimal theories $\mathcal{M}(A_{g-2},\mathcal{G})$, as classified in [7]. Based on this and further evidence, we conclude that the integrable boundary conditions obtained here provide lattice realisations of the $\mathcal{M}(A_{g-2},\mathcal{G})$ conformal boundary conditions.

In Section 5, we briefly discuss ways in which the formalism of this paper could be generalised.

2. Relevant Results on the Temperley-Lieb Algebra

In this section, we list and obtain various results on the Temperley-Lieb algebra. The defining relations of this algebra were first identified in [34] and the formalism used here is largely based on that of [35, 36, 37].

Our primary objective in this section is to study operators in the abstract algebra, which, in certain representations of the algebra, correspond to bulk weights and boundary weights of a lattice model. In particular, motivated by the procedure of [4], we shall construct certain boundary operators. This procedure involves fusion, which can be regarded as a means whereby new fused operators satisfying the Yang-Baxter equation are formed by applying certain fusion operators to blocks of unfused operators. The process of fusion was introduced in [38] and first used in the context of the Temperley-Lieb algebra in [35, 36].

2.1 The Temperley-Lieb Algebra; General Notation

The Temperley-Lieb algebra $\mathcal{T}(L,\lambda)$, with $L \in \mathbb{Z}_{\geq 0}$ and $\lambda \in \mathbb{C}$, is generated by the identity I together with operators $e_1, \ldots, e_L$ which satisfy

$$\begin{aligned} e_j^2 &= 2\cos\lambda\, e_j \\ e_j\, e_k\, e_j &= e_j, \quad |j-k| = 1 \\ e_j\, e_k &= e_k\, e_j, \quad |j-k| > 1\,. \end{aligned} \tag{2.1}$$

The various operators to be studied in Section 2 will all be elements of $\mathcal{T}(L,\lambda)$ for some fixed L and λ.

Throughout this paper, we shall use the notation

$$s_r(u) \;=\; \begin{cases} \dfrac{\sin(r\lambda+u)}{\sin\lambda}\,, & \lambda/\pi \notin \mathbb{Z} \\ (-1)^{(r+1)\lambda/\pi}\,(r+u), & \lambda/\pi \in \mathbb{Z}\,, \end{cases} \tag{2.2}$$

for any $r \in \mathbb{Z}$ and $u \in \mathbb{C}$, with λ being the same constant as in $\mathcal{T}(L,\lambda)$.

We note that the second case in (2.2) is simply a limiting case of the first,

$$s_r(u)\Big|_{\lambda/\pi\in\mathbb{Z}} \;=\; \lim_{\lambda'\to\lambda} \frac{\sin(r\lambda'+(\lambda'-\lambda)u)}{\sin\lambda'}\,, \tag{2.3}$$

so that in proving identities satisfied by these functions it is often sufficient to consider only the first case.

We shall also denote, for any $r \in \mathbb{Z}$,

$$S_r = s_r(0)\,. \tag{2.4}$$

We see, as examples, that for any λ,

$$S_0 = 0\,, \qquad S_1 = 1\,, \qquad S_2 = 2\cos\lambda\,. \tag{2.5}$$

2.2 Face Operators

We now introduce face operators $X_j(u)$, for $j \in \{1, \ldots, L\}$ and $u \in \mathbb{C}$, as

$$X_j(u) \;=\; s_1(-u)\, I \;+\; s_0(u)\, e_j\,. \tag{2.6}$$

These operators correspond in a lattice model to the bulk Boltzmann weights of faces of the lattice, and in this context λ and u are respectively known as the crossing and spectral parameters.

We shall represent the face operators diagrammatically as

$X_j(u) \quad =$ 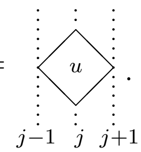 . (2.7)

From the Temperley-Lieb relations (2.1) and properties of the functions (2.2), it follows that the face operators satisfy the operator form of the Yang-Baxter equation,

$$X_j(u)\; X_{j+1}(u{+}v)\; X_j(v) \quad = \quad X_{j+1}(v)\; X_j(u{+}v)\; X_{j+1}(u)$$

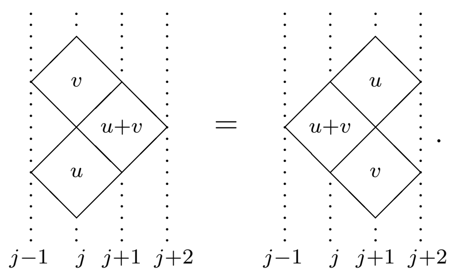 . (2.8)

We see that the face operators also satisfy the commutation relation

$$X_j(u)\, X_j(v) \;=\; X_j(v)\, X_j(u) \tag{2.9}$$

and the operator form of the inversion relation

$$X_j(-u)\, X_j(u) \;=\; s_1(-u)\, s_1(u)\, I\,. \tag{2.10}$$

2.3 Fusion Operators

We now proceed to consider some aspects of the process of fusion. In particular, we shall state some important properties of fusion operators. The proofs of these, or similar, properties can be found in [35, 36].

In general, fusion levels correspond to integrable representations of an affine Lie algebra. In the case considered here, this algebra is $\hat{s\ell}(2)$ and the fusion levels are labelled by a single integer $r \in \{1, 2, \ldots, g\}$, where the maximum fusion level g depends on λ according to

$$g \;=\; \begin{cases} k, & \lambda = h\pi/k, \;\; h \text{ and } k \text{ coprime integers}, \;\; k > 1 \\ \infty, & \text{otherwise}\,. \end{cases} \tag{2.11}$$

We now introduce fusion operators P_j^r, for $r \in \{1, \ldots, \min(g, L{+}2)\}$ and $j \in \{1, \ldots, L{+}3{-}r\}$, these being defined recursively by

$$\begin{aligned} P_j^1 \;&=\; P_j^2 \;=\; I \\ P_j^r \;&=\; \frac{1}{S_{r-1}}\, P_{j+1}^{r-1}\, X_j(-(r{-}2)\lambda)\, P_{j+1}^{r-1}\,, \quad r \geq 3\,. \end{aligned} \tag{2.12}$$

We note that, for finite g, the restriction of fusion levels to $r \leq g$ is necessary in order to avoid $S_{r-1} = 0$ in the denominator in (2.12).

We shall represent the fusion operators diagrammatically as

$$P_j^r \quad = $$

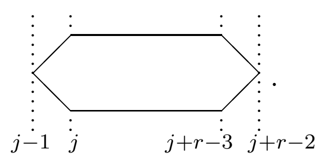

. (2.13)

In general, P_j^r can be expressed in terms of I and $e_j, \ldots, e_{j+r-3}$, the cases of the first few fusion levels being

$$\begin{aligned} P_j^1 \;=\; P_j^2 \;=\; I, \qquad P_j^3 \;=\; I - \frac{1}{S_2} e_j \\ P_j^4 \;=\; I - \frac{S_2}{S_3}(e_j + e_{j+1}) + \frac{1}{S_3}(e_j e_{j+1} + e_{j+1} e_j)\,. \end{aligned} \tag{2.14}$$

The fusion operators can also be expressed as

$$P_j^r \;=\; \prod_{k=2}^{r-1} S_k^{k-r}$$

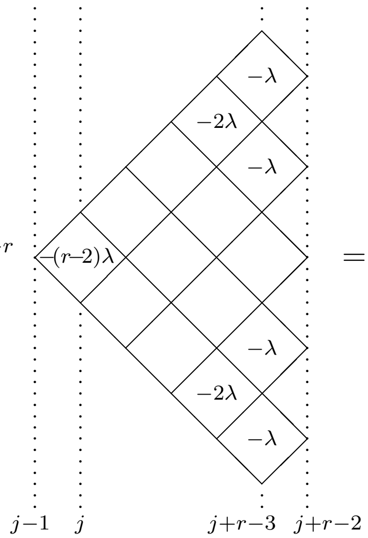

$$=\; \prod_{k=2}^{r-1} S_k^{k-r}$$

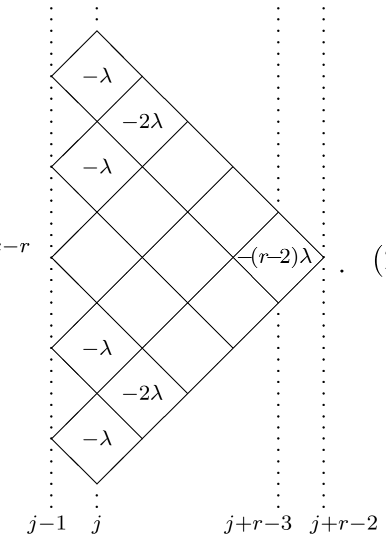

. (2.15)

A key property of the fusion operators is that they are projectors,

$$(P_j^r)^2 \;=\; P_j^r\,. \tag{2.16}$$

In fact, more generally, we have the property

$$P_{j'}^{r'}\,P_j^r \;=\; P_j^r\,P_{j'}^{r'} \;=\; P_j^r\,, \quad \text{if } 0 \le j'-j \le r-r'\,. \tag{2.17}$$

A useful case of this is $r'=3$, from which we have

$$e_{j'}\,P_j^r \;=\; P_j^r\,e_{j'} \;=\; 0, \quad \text{if } j \le j' \le j+r-3\,. \tag{2.18}$$

The fusion operators also satisfy the Hecke-like identity

$$S_{r-1}^2\,P_{j+1}^r\,P_j^r\,P_{j+1}^r \;-\; P_{j+1}^r \;=\; S_{r-1}^2\,P_j^r\,P_{j+1}^r\,P_j^r \;-\; P_j^r \;=\; S_{r-2}\,S_r\,P_j^{r+1}\,. \tag{2.19}$$

2.4 Fused Row Operators

We now introduce operators $Y_j^r(u)$ and $\tilde{Y}_j^r(u)$, for $r \in \{1,\ldots,\min(g-1,L+1)\}$ and $j \in \{1,\ldots,L+2-r\}$, which correspond to fused rows of faces. These operators are related to products of $r-1$ face operators, for $r \geq 2$, by

$$\begin{aligned}\prod_{k=1}^{r-2} s_k(-u)\, Y_j^r(u) &= P_{j+1}^r\, X_j(u-(r-2)\lambda)\, \ldots\, X_{j+r-3}(u-\lambda)\, X_{j+r-2}(u) \\ &= X_j(u)\, X_{j+1}(u-\lambda)\, \ldots\, X_{j+r-2}(u-(r-2)\lambda)\, P_j^r\end{aligned}$$

$=$ 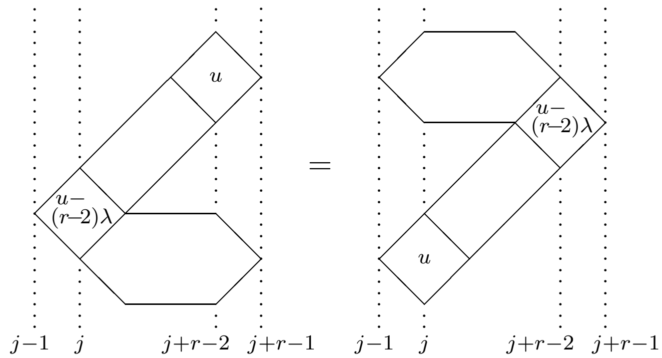 (2.20a)

and

$$\begin{aligned}\prod_{k=0}^{r-3} s_{-k}(-u)\, \tilde{Y}_j^r(u) &= P_j^r\, X_{j+r-2}(u)\, X_{j+r-3}(u+\lambda)\, \ldots\, X_j(u+(r-2)\lambda) \\ &= X_{j+r-2}(u+(r-2)\lambda)\, \ldots\, X_{j+1}(u+\lambda)\, X_j(u)\, P_{j+1}^r\end{aligned}$$

$=$ 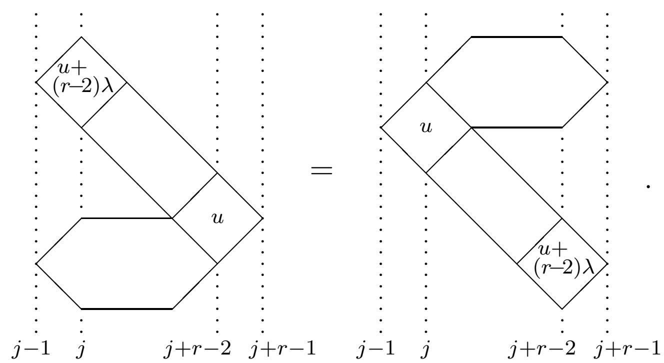 . (2.20b)

The second (or fourth) equalities in (2.20) imply the push-through relations

$$\begin{aligned}Y_j^r(u) &= P_{j+1}^r\, Y_j^r(u) = Y_j^r(u)\, P_j^r \\ \tilde{Y}_j^r(u) &= P_j^r\, \tilde{Y}_j^r(u) = \tilde{Y}_j^r(u)\, P_{j+1}^r\,,\end{aligned} \tag{2.21}$$

and can be derived using (2.15) and repeated application of (2.8).

The fused row operators can be written in terms of fusion operators as

$$\begin{aligned} Y^r_j(u) &= S_{r-1}\, s_1(u)\, P^r_{j+1}\, P^r_j \;-\; S_r\, s_0(u)\, P^{r+1}_j \\ \tilde{Y}^r_j(u) &= S_{r-1}\, s_{r-1}(u)\, P^r_j\, P^r_{j+1} \;-\; S_n\, s_{r-2}(u)\, P^{r+1}_j\,. \end{aligned} \tag{2.22}$$

The equivalence of (2.20) and (2.22) follows from several of the properties of fusion operators listed in Section 2.3.

We note, as examples, that for the first two fusion levels,

$$Y^1_j(u) \;=\; -s_0(u)\, I, \quad \tilde{Y}^1_j(u) \;=\; s_1(-u)\, I, \quad Y^2_j(u) \;=\; \tilde{Y}^2_j(u) \;=\; X_j(u)\,. \tag{2.23}$$

An important property of the fused row operators is that they satisfy the mixed Yang-Baxter equations,

$$X_j(u-v)\, Y^r_{j+1}(u)\, Y^r_j(v) \;=\; Y^r_{j+1}(v)\, Y^r_j(u)\, X_{j+r-1}(u-v) \tag{2.24}$$

$$X_{j+r-1}(u-v)\, \tilde{Y}^r_j(u)\, \tilde{Y}^r_{j+1}(v) \;=\; \tilde{Y}^r_j(v)\, \tilde{Y}^r_{j+1}(u)\, X_j(u-v) \tag{2.25}$$

$$Y^r_j(u)\, X_{j+r-1}(u+v)\, \tilde{Y}^r_j(v) \;=\; \tilde{Y}^r_{j+1}(v)\, X_j(u+v)\, Y^r_{j+1}(u)\,. \tag{2.26}$$

These equations can be obtained using (2.20) and repeated application of (2.8).

They fused row operators also satisfy the product identities

$$\begin{aligned} Y^r_j(u)\, \tilde{Y}^r_j(v) &= s_1(u)\, s_{r-1}(v)\, P^r_{j+1} \;-\; S_r\, s_0(u+v)\, P^{r+1}_j \\ \tilde{Y}^r_j(u)\, Y^r_j(v) &= s_{r-1}(u)\, s_1(v)\, P^r_j \;-\; S_r\, s_0(u+v)\, P^{r+1}_j\,, \end{aligned} \tag{2.27}$$

these being most easily derived using (2.22) and properties of the fusion operators.

2.5 Boundary Operators

We now introduce boundary operators $K^r_j(u,\xi)$, with $\xi \in \mathbb{C}$, as products of two fused row operators,

$$K^r_j(u,\xi) \;=\; -\,Y^r_j(u-\lambda-\xi)\, \tilde{Y}^r_j(u+\lambda+\xi)\,. \tag{2.28}$$

These operators correspond in a lattice model to boundary Boltzmann weights, and in this context ξ is a boundary field parameter.

From (2.27), we see that the boundary operators can be written in terms of fusion operators as

$$K^r_j(u,\xi) \;=\; s_0(\xi-u)\,s_r(\xi+u)\,P^r_{j+1} \;+\; S_r\,s_0(2u)\,P^{r+1}_j\,. \tag{2.29}$$

An alternative expression, which follows using (2.12) on the second term on the right side of (2.29), is

$$K^r_j(u,\xi) \;=\; s_0(\xi+u)\,s_r(\xi-u)\,P^{r+1}_j \;+\; \frac{S_{r-1}}{S_r}\,s_0(\xi-u)\,s_r(\xi+u)\,P^r_{j+1}\,e_j\,P^r_{j+1}\,. \tag{2.30}$$

We see, as examples, that for the first two fusion levels,

$$K^1_j(u,\xi) \;=\; s_0(\xi{+}u)\,s_1(\xi{-}u)\,I, \quad K^2_j(u,\xi) \;=\; s_0(\xi{+}u)\,s_2(\xi{-}u)\,I \,-\, s_0(2u)\,e_j. \tag{2.31}$$

The key property of the face and boundary operators is that they satisfy the operator form of the boundary Yang-Baxter equation,

$$\begin{aligned} &X_j(u-v)\,K^r_{j+1}(u,\xi)\,X_j(u+v)\,K^r_{j+1}(v,\xi) \;= \\ &\qquad\qquad K^r_{j+1}(v,\xi)\,X_j(u+v)\,K^r_{j+1}(u,\xi)\,X_j(u-v)\,. \end{aligned} \tag{2.32}$$

This can be proved by substituting (2.28) into the left side of (2.32), using (2.26) followed by (2.24) to bring $X_j(u-v)$ adjacent to $X_j(u+v)$, interchanging the order of these face operators using (2.9), and then using (2.25) followed by (2.26) to give the right side of (2.32).

In terms of the construction procedure of [4], the boundary operators $K^r_j(u,\xi)$ can be considered as a family of solutions, one solution for each value of r, of (2.32) with given $X_j(u)$, these solutions having been constructed by starting with the identity solution of (2.32) and adding a fused double row of faces of width $r-1$.

The boundary operators also satisfy the operator form of the boundary inversion relation,

$$K^r_j(u,\xi)\,K^r_j(-u,\xi) \;=\; s_0(\xi-u)\,s_0(\xi+u)\,s_r(\xi-u)\,s_r(\xi+u)\,P^r_{j+1}\,, \tag{2.33}$$

this being most easily obtained using (2.29) and properties of the fusion operators.

3. Lattice Models Based on Graphs

In this section, we consider representations of the Temperley-Lieb algebra involving a graph $\mathcal{G}$ and their associated lattice models. Our general treatment is based on that introduced in [8, 28] and, when considering fusion for these models, our approach is also motivated by certain results of [39, 40, 41, 42].

In the lattice model based on $\mathcal{G}$, a spin is attached to each site of a two-dimensional square lattice, with the possible states of each spin being the nodes of $\mathcal{G}$ and there being a lattice adjacency condition stipulating that, in any assignment of spin states to the lattice, the states on each pair of nearest-neighbour sites must correspond to an edge of $\mathcal{G}$. These models are interaction-round-a-face models, so that a bulk Boltzmann weight is associated with each set of four spin states adjacent around a square face. Here, we shall also obtain and use sets of boundary weights, each of these weights being associated with three adjacent spin states. The partition function of the model on a cylinder is then the sum, over all possible spin assignments, of products of Boltzmann weights, with each square face in the bulk of the lattice contributing a bulk weight and each non-overlapping triplet of neighbouring sites on the boundaries contributing a boundary weight.

The key property of the boundary weights obtained in this section is that they satisfy the boundary Yang-Baxter equation for interaction-round-a-face models. This equation was first used in [31, 43] and is based on the so-called reflection equation introduced in [44]. However, we note that, due to the dependence of each boundary weight used here on two fusion indices, the form of these weights and that of the boundary Yang-Baxter equation are somewhat more general than that used in all previous studies. We shall show that a further important property of the three-spin boundary weights used here is that, at a certain point, they simultaneously decompose into more natural two-spin boundary edge weights.

Finally, using these and other local properties of the bulk and boundary weights, we shall identify various symmetry properties of the partition function and transfer matrices, including the invariance of the partition function under interchanging parts or all of the left and right boundaries, and the facts that the transfer matrices form a commuting family, with, at certain points, all of their eigenvalues being nonnegative.

3.1 Graphs and Paths

Throughout Section 3, we shall be considering a finite graph $\mathcal{G}$ with an associated adjacency matrix G. We require that $\mathcal{G}$ contain only unoriented, single bonds, implying that G is symmetric and that each of its nonzero entries is 1.

We also require that $\mathcal{G}$ be connected. Perron-Frobenius theory then implies that G has a unique maximum eigenvalue with an associated eigenvector whose entries are all positive.

We shall denote the set of all r-point paths on $\mathcal{G}$, for $r \in \mathbb{Z}_{\geq 1}$, by $\mathcal{G}^r$; that is,

$$\mathcal{G}^r \;=\; \Big\{(a_0,\ldots,a_{r-1})\,\Big|\,a_j \in \mathcal{G},\; \prod_{j=0}^{r-2} G_{a_j a_{j+1}} = 1\Big\}\,. \tag{3.1}$$

We note that $\mathcal{G}^1$ corresponds to the set of nodes of $\mathcal{G}$ and that $\mathcal{G}^2$ is the set of edges of $\mathcal{G}$.

We shall also denote the set of all r-point paths between a and b in $\mathcal{G}$ by $\mathcal{G}^r_{ab}$; that is,

$$\mathcal{G}^r_{ab} \;=\; \Big\{(a_0,\ldots,a_{r-1}) \in \mathcal{G}^r\,\Big|\,a_0 = a,\; a_{r-1} = b\Big\}\,. \tag{3.2}$$

It follows that

$$|\mathcal{G}^r_{ab}| \;=\; (G^{r-1})_{ab}\,. \tag{3.3}$$

3.2 Graph Representations of the Temperley-Lieb Algebra

A graph representation involving $\mathcal{G}$ of the Temperley-Lieb algebra $\mathcal{T}(L,\lambda)$ exists for each λ for which $2\cos\lambda$ is an eigenvalue of G with an associated eigenvector ψ whose entries are all nonzero; that is, for which

$$\sum_{b\,\in\,\mathcal{G}} G_{ab}\,\psi_b \;=\; 2\cos\lambda\;\psi_a \quad\text{and}\quad \psi_a \neq 0\,, \quad \text{for each } a \in \mathcal{G}. \tag{3.4}$$

There is always at least one such case, namely that provided by the Perron-Frobenius eigenvalue and eigenvector. We shall assume, throughout the rest of Section 3, that λ and ψ are fixed.

The elements of this graph representation are matrices with rows and columns labelled by the paths of $\mathcal{G}^{L+2}$, with the generators e_j being defined by

$$e_{j\,(a_0,\ldots,a_{L+1}),(b_0,\ldots,b_{L+1})} \;=\; \frac{\psi_{a_j}^{1/2}\;\psi_{b_j}^{1/2}}{\psi_{a_{j-1}}}\;\delta_{a_{j-1}a_{j+1}}\prod_{\substack{k=0\\k\neq j}}^{L+1}\delta_{a_kb_k}\,. \tag{3.5}$$

It follows straightforwardly that the defining relations (2.1) of $\mathcal{T}(L,\lambda)$ are satisfied, with the first relation depending on (3.4).

We see that each e_j is a symmetric matrix. Also, since G is symmetric, $\cos\lambda$ must be real and each ψ_a can, and will, be assumed to be real. However, whether the entries of the e_j are real will depend on the signs of the ψ_a.

3.3 Bulk Weights

We now proceed to consider the lattice model based on $\mathcal{G}$ and associated with the adjacency matrix eigenvalue and eigenvector given by (3.4).

The bulk weights for this model are given explicitly, for each $(a,b,c,d,a)\in\mathcal{G}^5$, by

$$W\!\left(\begin{matrix}d & c\\ a & b\end{matrix}\,\middle|\,u\right) \;=\; s_1(-u)\,\delta_{ac} \;+\; \frac{s_0(u)\;\psi_a^{1/2}\;\psi_c^{1/2}}{\psi_b}\,\delta_{bd}\,, \tag{3.6}$$

where u is the spectral parameter and λ, on which s and ψ depend through (2.2) and (3.4), is the crossing parameter. The spectral parameter can be considered as a measure of anisotropy, with $u=\lambda/2$ being an isotropic point and $u=0$ and $u=\lambda$ being completely anisotropic points.

We shall represent the bulk weights diagrammatically as

$$W\!\left(\begin{matrix}d & c\\ a & b\end{matrix}\,\middle|\,u\right) \quad = \tag{3.7}$$

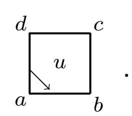

These bulk weights are related to the face operators (2.6) by

$$W\!\left(\begin{matrix}d & c\\ a & b\end{matrix}\,\middle|\,u\right) \;=\; X_1(u)_{(d,a,b),(d,c,b)}\,, \tag{3.8}$$

where $X_1(u)$ is taken in the graph representation of $\mathcal{T}(1,\lambda)$.

We see that the bulk weights satisfy reflection symmetry,

$$W\left(\begin{matrix} d & c \\ a & b \end{matrix}\,\middle|\, u\right) \;=\; W\left(\begin{matrix} b & c \\ a & d \end{matrix}\,\middle|\, u\right) \;=\; W\left(\begin{matrix} d & a \\ c & b \end{matrix}\,\middle|\, u\right), \tag{3.9}$$

crossing symmetry,

$$W\left(\begin{matrix} d & c \\ a & b \end{matrix}\,\middle|\, u\right) \;=\; \frac{\psi_a^{1/2}\,\psi_c^{1/2}}{\psi_b^{1/2}\,\psi_d^{1/2}}\, W\left(\begin{matrix} c & d \\ b & a \end{matrix}\,\middle|\, \lambda{-}u\right), \tag{3.10}$$

and the anisotropy property

$$W\left(\begin{matrix} d & c \\ a & b \end{matrix}\,\middle|\, 0\right) \;=\; \delta_{ac}\,. \tag{3.11}$$

It follows from (2.8) and (2.10) that the bulk weights also satisfy the Yang-Baxter equation,

$$\sum_{\substack{g\,\in\,\mathcal{G} \\ (G_{bg}G_{dg}G_{fg}=1)}} W\left(\begin{matrix} f & g \\ a & b \end{matrix}\,\middle|\, u{-}v\right) W\left(\begin{matrix} g & d \\ b & c \end{matrix}\,\middle|\, u\right) W\left(\begin{matrix} f & e \\ g & d \end{matrix}\,\middle|\, v\right) \;=\;$$

$$\sum_{\substack{g\,\in\,\mathcal{G} \\ (G_{ag}G_{cg}G_{eg}=1)}} W\left(\begin{matrix} a & g \\ b & c \end{matrix}\,\middle|\, v\right) W\left(\begin{matrix} f & e \\ a & g \end{matrix}\,\middle|\, u\right) W\left(\begin{matrix} e & d \\ g & c \end{matrix}\,\middle|\, u{-}v\right) \tag{3.12}$$

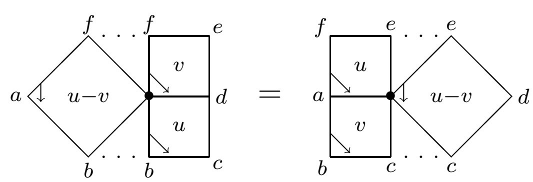

for each $(a,b,c,d,e,f,a) \in \mathcal{G}^7$, and the inversion relation

$$\sum_{\substack{e\,\in\,\mathcal{G} \\ (G_{be}G_{de}=1)}} W\left(\begin{matrix} d & e \\ a & b \end{matrix}\,\middle|\, -u\right) W\left(\begin{matrix} d & c \\ e & b \end{matrix}\,\middle|\, u\right) \;=\; \tag{3.13}$$

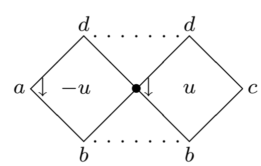

$$=\; s_1(u)\, s_1(-u)\, \delta_{ac}\,,$$

for each $(a,b,c,d,a) \in \mathcal{G}^5$. In these and all subsequent diagrams, solid circles are used to indicate spins whose states are summed over and dotted lines are used to connect identical spins.

3.4 Fusion Matrices, Fused Adjacency Matrices and Fusion Vectors

We now consider various objects related to the process of fusion in lattice models based on graphs.

We first introduce, for each $r \in \{1,\ldots,g\}$ and $a,b \in \mathcal{G}$ satisfying $(G^{r-1})_{ab} > 0$, a fusion matrix $P^r(a,b)$ with rows and columns labelled by the paths of $\mathcal{G}^r_{ab}$ and entries given by

$$P^r(a,b)_{(a,c_1,\ldots,c_{r-2},b),(a,d_1,\ldots,d_{r-2},b)} \;=\; \begin{cases} 1\,, & r=1 \\ P^r_1{}_{(a,c_1,\ldots,c_{r-2},b),(a,d_1,\ldots,d_{r-2},b)}\,, & r=2,\ldots,g\,, \end{cases} \tag{3.14}$$

where the fusion operator P^r_1 is defined by (2.12) and taken in the graph representation of $\mathcal{T}(r-2,\lambda)$.

It follows from (2.16) that each fusion matrix is a projector,

$$P^r(a,b)^2 \;=\; P^r(a,b)\,. \tag{3.15}$$

It also follows, from the symmetry of the generators e_j, that each fusion matrix is symmetric,

$$P^r(a,b)^T \;=\; P^r(a,b) \tag{3.16}$$

and, from (2.15), that a and b can interchanged according to

$$P^r(a,b)_{(a,c_1,\ldots,c_{r-2},b),(a,d_1,\ldots,d_{r-2},b)} \;=\; P^r(b,a)_{(b,c_{r-2},\ldots,c_1,a),(b,d_{r-2},\ldots,d_1,a)}\,. \tag{3.17}$$

We note that the fusion matrices also satisfy more general projection-type relations corresponding to those, (2.17), satisfied by the fusion operators.

We next introduce fused adjacency matrices, $F^1,\ldots,F^g$, which are defined by the $\hat{s\ell}(2)$ recursion,

$$F^1 \;=\; I\,; \qquad F^2 \;=\; G\,; \qquad F^r \;=\; G\,F^{r-1} \,-\, F^{r-2}\,, \quad r=3,\ldots,g\,. \tag{3.18}$$

We see that each fused adjacency matrix is a polynomial in G and hence that the set of these matrices is mutually commuting. In fact, the polynomial form is given by the Type II Chebyshev polynomials $\mathcal{U}_r$,

$$F^r = \mathcal{U}_{r-1}(G/2)\,. \tag{3.19}$$

We note that at a few places in Section 4, we shall be considering the fused adjacency matrices of two different graphs and in these cases we shall explicitly indicate the dependence on the graph as $F(\mathcal{G})^r$.

The main relevance of the fused adjacency matrices at this point is that their entries give the ranks of the fusion matrices, according to

$$F^r_{ab} = \begin{cases} 0\,, & (G^{r-1})_{ab} = 0 \\ \mathrm{rank} P^r(a,b)\,, & (G^{r-1})_{ab} > 0\,. \end{cases} \tag{3.20}$$

This result can be proved by defining matrices $\tilde{F}^r$ with entries $\tilde{F}^r_{ab}$ given by the right side of (3.20) and showing that these matrices satisfy relations (3.18), so that $\tilde{F}^r = F^r$. Showing that $\tilde{F}^r$ satisfy the initial conditions of (3.18) is straightforward. Meanwhile, showing that $\tilde{F}^r$ satisfy the recursion relation of (3.18) can be done by using the fact that the rank of any projector is given by its trace (since by idempotence each eigenvalue is either 0 or 1, the rank is the number of eigenvalues which are 1 and the trace is the sum of eigenvalues) and then using definitions (2.6), (3.5) and (3.14), the recursion relation of (2.12), which is needed twice, relations (2.16) and (3.4), and general properties of the trace and of the numbers S_r.

We note that (3.20) also implies that F^r_{ab} are nonnegative integers and that each F^r can therefore be viewed as an adjacency matrix. In fact, the property that the entries of F^r are integers follows immediately from the properties that the entries of G are integers and that each F^r is a polynomial, with integer coefficients, in G. However, the property that the entries of F^r are also nonnegative is less trivial and depends on the additionally-assumed properties of G, such as its being symmetric, and on the restriction $r \leq g$.

We now make the assumption, which will apply from here on, that ψ is the Perron-Frobenius eigenvector, so that

$$\psi_a > 0 \text{ for each } a \in \mathcal{G}. \tag{3.21}$$

This implies that each $P^r(a,b)$ is real symmetric and therefore that it can be decomposed using F^r_{ab} real orthonormal eigenvectors with eigenvalue 1. We shall denote, for $r \in \{1,\ldots,g\}$ and $a,b \in \mathcal{G}$ satisfying $F^r_{ab} > 0$, such eigenvectors as $U^r(a,b)_\alpha$, with $\alpha = 1,\ldots,F^r_{ab}$, and refer to these as fusion vectors. The decomposition and orthonormality are then

$$\sum_{\alpha=1}^{F^r_{ab}} U^r(a,b)_\alpha \; U^r(a,b)_\alpha^{\,T} \;=\; P^r(a,b) \tag{3.22}$$

and

$$U^r(a,b)_\alpha^{\,T} \; U^r(a,b)_{\alpha'} \;=\; \delta_{\alpha\alpha'}\,, \tag{3.23}$$

or, more explicitly,

$$\sum_{\alpha=1}^{F^r_{ab}} U^r(a,b)_{\alpha,(a,c_1,\ldots,c_{r-2},b)} \; U^r(a,b)_{\alpha,(a,d_1,\ldots,d_{r-2},b)} \;=\; P^r(a,b)_{(a,c_1,\ldots,c_{r-2},b),(a,d_1,\ldots,d_{r-2},b)}$$

and

$$\sum_{(a,c_1,\ldots,c_{r-2},b)\,\in\,\mathcal{G}^r_{ab}} U^r(a,b)_{\alpha,(a,c_1,\ldots,c_{r-2},b)} \; U^r(a,b)_{\alpha',(a,c_1,\ldots,c_{r-2},b)} \;=\; \delta_{\alpha\alpha'}\,.$$

We note, as examples, that for the first two fusion levels,

$$P^1(a,a)_{(a),(a)} \;=\; |U^1(a,a)_{1,(a)}| \;=\; 1\,, \quad \text{for each } a \in \mathcal{G}\,, \tag{3.24}$$

and

$$P^2(a,b)_{(a,b),(a,b)} \;=\; |U^2(a,b)_{1,(a,b)}| \;=\; 1\,, \quad \text{for each } (a,b) \in \mathcal{G}^2\,. \tag{3.25}$$

We shall assume that a specific choice of $U^r(a,b)_\alpha$ has been made. All other possible choices are then given by transformations,

$$U^r(a,b)_\alpha \;\mapsto\; \sum_{\alpha'=1}^{F^r_{ab}} R^r(a,b)_{\alpha\alpha'}\, U^r(a,b)_{\alpha'}\,, \tag{3.26}$$

where $R^r(a,b)$ is an orthonormal matrix,

$$\sum_{\alpha''=1}^{F^r_{ab}} R^r(a,b)_{\alpha\alpha''}\, R^r(a,b)_{\alpha'\alpha''} \;=\; \delta_{\alpha\alpha'}\,. \tag{3.27}$$

We shall see that all of the lattice model properties of interest will be invariant under such transformations and thus independent of the choice of fusion vectors.

3.5 Boundary Weights

We now use the boundary operators (2.28) to obtain a set of boundary Boltzmann weights for the lattice model for each pair (r,a), where $r \in \{1,\ldots,g{-}1\}$ is a fusion level and a is a node of $\mathcal{G}$. It is thus natural to regard these pairs as labelling the boundary conditions,

$$\Big\{\text{boundary conditions}\Big\} \;\longleftrightarrow\; \Big\{(r,a)\mid r\in\{1,\ldots,g{-}1\},\ a\in\mathcal{G}\Big\}\,. \tag{3.28}$$

These (r,a) boundary weights are given, for each $(b,c,d)\in\mathcal{G}^3$ with $F^r_{ba}\,F^r_{da}>0$ and $\beta\in\{1,\ldots,F^r_{ba}\}$, $\delta\in\{1,\ldots,F^r_{da}\}$, by

$$\begin{aligned} B^{ra}\!\left(c\;\begin{matrix} d & \delta\\ b & \beta\end{matrix}\,\middle|\,u,\xi\right) &= \\ \frac{\psi_c^{1/2}}{s_0(2\xi)\,(\psi_b\,\psi_d)^{1/4}} &\sum_{\substack{(b,e_1,\ldots,e_{r-2},a)\,\in\,\mathcal{G}^r_{ba}\\ (d,f_1,\ldots,f_{r-2},a)\,\in\,\mathcal{G}^r_{da}}} U^r(b,a)_{\beta,(b,e_1,\ldots,e_{r-2},a)}\,U^r(d,a)_{\delta,(d,f_1,\ldots,f_{r-2},a)} \\ &\qquad\times K_1^r(u,\xi)_{(c,b,e_1,\ldots,e_{r-2},a),(c,d,f_1,\ldots,f_{r-2},a)}\,, \end{aligned} \tag{3.29}$$

where $K_1^r(u,\xi)$ is taken in the graph representation of $\mathcal{T}(r{-}1,\lambda)$ and ξ corresponds to a boundary field. We shall represent the boundary weights diagrammatically as

$$B^{ra}\!\left(c\;\begin{matrix} d & \delta\\ b & \beta\end{matrix}\,\middle|\,u,\xi\right) \;=\; \tag{3.30}$$

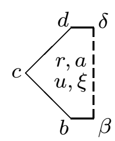

.

We see that

$$\text{number of } (r,a) \text{ boundary weights} \;=\; \big((F^r)^2\,G^2\big)_{aa}\,. \tag{3.31}$$

We shall refer to a boundary weight (3.29) as being of diagonal type if $b=d$ and $\beta=\delta$ and of nondiagonal type otherwise, and we note that in the majority of previous studies involving such boundary weights, only diagonal weights were considered.

We also note, as an example, that the $(1,a)$ boundary weights are all diagonal and given by

$$B^{1a}\!\left(c\;\begin{matrix} a & 1\\ a & 1\end{matrix}\,\middle|\,u,\xi\right) \;=\; \frac{s_0(\xi{+}u)\,s_1(\xi{-}u)\,\psi_c^{1/2}}{s_0(2\xi)\,\psi_a^{1/2}}\,. \tag{3.32}$$

A $(1,a)$ boundary condition is thus one in which the state of every alternate boundary spin is fixed to be a, while each other boundary spin, whose state can be any c adjacent to a on $\mathcal{G}$, is associated with a weight proportional to $\psi_c^{1/2}$. We shall refer to such a boundary condition, in which the state of every alternate boundary spin is fixed, as semi-fixed.

We now find that the boundary weights can also be expressed as

$$B^{ra}\!\left(c\;\begin{matrix} d & \delta \\ b & \beta \end{matrix}\;\middle|\; u,\xi\right) \;=\; -\Big(s_0(2\xi)\prod_{k=1}^{r-2} s_{-k-1}(u-\xi)\,s_k(u+\xi)\Big)^{-1}\times$$

$$U^r(d,a)_{\delta,(d,f_1,f_2,\ldots,f_{r-2},a)}$$

$$\frac{\psi_d^{1/4}\,\psi_g^{1/2}}{\psi_b^{1/4}\,\psi_a^{1/2}} \qquad (3.33)$$

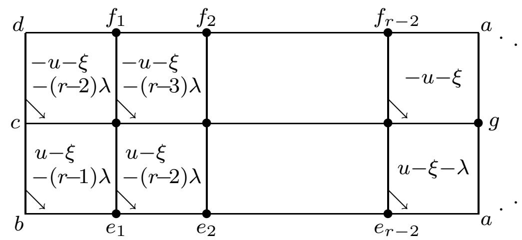

$$U^r(b,a)_{\beta,(b,e_1,e_2,\ldots,e_{r-2},a)}$$

this following straightforwardly from (2.28), (2.20), (3.14), (3.6), (3.10), (3.22) and (3.23). In this form, we see that the (r,a) boundary weights can be considered as having been constructed by starting on the right at node a, essentially with the level 1 boundary weights (3.32), and adding a fused double row of bulk weights of width $r-1$.

The boundary weights, together with the bulk weights (3.6), satisfy the boundary

Yang-Baxter equation,

$$
\begin{aligned}
&\sum_{\substack{(g,h)\,\in\,\mathcal{G}^2\\(G_{dg}G_{bg}G_{he}F^r_{ha}>0)}}\ \sum_{\gamma=1}^{F^r_{ha}} W\!\left(\begin{matrix} d & g\\ c & b\end{matrix}\,\middle|\, u-v\right) B^{ra}\!\left(g\ \begin{matrix} h & \gamma\\ b & \beta\end{matrix}\,\middle|\, u,\xi\right) \times\\
&\qquad\qquad W\!\left(\begin{matrix} e & h\\ d & g\end{matrix}\,\middle|\, \lambda-u-v\right) B^{ra}\!\left(e\ \begin{matrix} f & \delta\\ h & \gamma\end{matrix}\,\middle|\, v,\xi\right) =\\
&\sum_{\substack{(g,h)\,\in\,\mathcal{G}^2\\(G_{ch}G_{gf}G_{gd}F^r_{ha}>0)}}\ \sum_{\gamma=1}^{F^r_{ha}} B^{ra}\!\left(c\ \begin{matrix} h & \gamma\\ b & \beta\end{matrix}\,\middle|\, v,\xi\right) W\!\left(\begin{matrix} g & h\\ d & c\end{matrix}\,\middle|\, \lambda-u-v\right) \times\\
&\qquad\qquad B^{ra}\!\left(g\ \begin{matrix} f & \delta\\ h & \gamma\end{matrix}\,\middle|\, u,\xi\right) W\!\left(\begin{matrix} f & g\\ e & d\end{matrix}\,\middle|\, u-v\right)
\end{aligned}
\tag{3.34}
$$

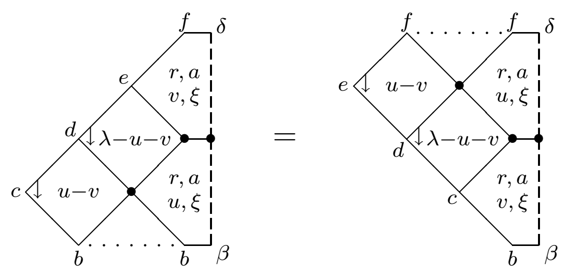

,

for each $(b,c,d,e,f)\in\mathcal{G}^5$ with $F^r_{ba}\,F^r_{fa}>0$ and $\beta\in\{1,\ldots,F^r_{ba}\}$, $\delta\in\{1,\ldots,F^r_{fa}\}$. This equation can be verified by expressing the bulk and boundary weights in terms of bulk and boundary operators, using (3.6) and (3.29), and applying the operator form of the boundary Yang-Baxter equation, (2.32). In doing this, the fusion matrix which is formed on the interior of each side of the equation by the sum on γ and (3.22) can be moved to the exterior by expressing the fusion matrices in terms of fusion operators using (3.14) and the boundary operators in terms of fused row operators using (2.28) and applying the push-through relations (2.21). Meanwhile, the orientation of the central bulk weights on each side of (3.34) can be changed to that required for (2.32) by using crossing symmetry (3.10), with the eigenvector entries from (3.10) cancelling where needed with those introduced explicitly through (3.29).

We note that the boundary Yang-Baxter equation (3.34) is still satisfied after renormalisation of the boundary weights,

$$B^{ra}\!\left(c \begin{array}{cc} d & \delta \\ b & \beta \end{array} \middle| \, u,\xi \right) \;\mapsto\; f^{ra}(u,\xi)\; B^{ra}\!\left(c \begin{array}{cc} d & \delta \\ b & \beta \end{array} \middle| \, u,\xi \right) , \tag{3.35}$$

where f^{ra} are arbitrary functions. It is also still satisfied after gauge transformations of the boundary weights,

$$B^{ra}\!\left(c \begin{array}{cc} d & \delta \\ b & \beta \end{array} \middle| \, u,\xi \right) \;\mapsto\; \sum_{\beta'=1}^{F^r_{ba}} \sum_{\delta'=1}^{F^r_{da}} S^{ra}(b)_{\beta\beta'}\; S^{ra}(d)_{\delta\delta'}\; B^{ra}\!\left(c \begin{array}{cc} d & \delta' \\ b & \beta' \end{array} \middle| \, u,\xi \right) , \tag{3.36}$$

where $S^{ra}(e)$ are arbitrary orthonormal matrices,

$$\sum_{\alpha''=1}^{F^r_{ea}} S^{ra}(e)_{\alpha\alpha''}\; S^{ra}(e)_{\alpha'\alpha''} \;=\; \delta_{\alpha\alpha'} \,. \tag{3.37}$$

Indeed, a transformation (3.26) of the fusion vectors simply induces a gauge transformation of the boundary weights with

$$S^{ra}(e) = R^r(e,a)\,. \tag{3.38}$$

In addition to the boundary Yang-Baxter equation, some other important local relations satisfied by the boundary weights are boundary reflection symmetry,

$$B^{ra}\!\left(c \begin{array}{cc} d & \delta \\ b & \beta \end{array} \middle| \, u,\xi \right) \;=\; B^{ra}\!\left(c \begin{array}{cc} b & \beta \\ d & \delta \end{array} \middle| \, u,\xi \right) , \tag{3.39}$$

boundary crossing symmetry,

$$\begin{aligned} &\sum_{(b,e,d)\,\in\,\mathcal{G}^3_{bd}} W\!\left(\begin{array}{cc} d & e \\ c & b \end{array} \middle| \; 2u-\lambda \right) B^{ra}\!\left(e \begin{array}{cc} d & \delta \\ b & \beta \end{array} \middle| \, u,\xi \right) \\ &\qquad\qquad\qquad = \; s_0(2u)\; B^{ra}\!\left(c \begin{array}{cc} d & \delta \\ b & \beta \end{array} \middle| \, \lambda-u,\xi \right) , \end{aligned} \tag{3.40}$$

and the boundary inversion relation,

$$\begin{aligned} &\sum_{\substack{e\,\in\,\mathcal{G} \\ (G_{ce}F^r_{ea}>0)}} \sum_{\gamma=1}^{F^r_{ea}} \frac{(\psi_b\,\psi_d)^{1/4}\,\psi_e^{1/2}}{\psi_c}\; B^{ra}\!\left(c \begin{array}{cc} e & \gamma \\ b & \beta \end{array} \middle| \, u,\xi \right) B^{ra}\!\left(c \begin{array}{cc} d & \delta \\ e & \gamma \end{array} \middle| \, -u,\xi \right) \\ &\qquad\qquad = \; \frac{s_0(\xi-u)\; s_0(\xi+u)\; s_r(\xi-u)\; s_r(\xi+u)}{s_0(2\xi)^2}\; \delta_{bd}\; \delta_{\beta\delta}\,, \end{aligned} \tag{3.41}$$

for each $(b,c,d) \in \mathcal{G}^3$ with $F^r_{ba}\,F^r_{da} > 0$ and $\beta \in \{1,\ldots,F^r_{ba}\}$, $\delta \in \{1,\ldots,F^r_{da}\}$. Boundary reflection symmetry follows immediately from (3.29), boundary crossing symmetry can be proved by expressing the boundary weights in the form (3.33) and repeatedly applying the Yang-Baxter equation (3.12), and the boundary inversion relation follows from the operator form of the boundary inversion relation, (2.33).

3.6 Boundary Edge Weights

We now introduce boundary edge weights in terms of which the boundary weights of the previous section can be expressed.

We begin by defining, for each boundary condition (r,a), a set of boundary edges as

$$\mathcal{E}^{ra} \;=\; \{(b,c) \in \mathcal{G}^2 \mid F^r_{ba}\,F^{r+1}_{ca} > 0\}\,. \tag{3.42}$$

We note that the boundary edges are ordered pairs and that, in contrast to the graph's set of edges for which $(b,c) \in \mathcal{G}^2 \Leftrightarrow (c,b) \in \mathcal{G}^2$, the appearance of (b,c) in $\mathcal{E}^{ra}$ need not imply the appearance of (c,b) in $\mathcal{E}^{ra}$.

The (r,a) boundary edge weights are now given, for each $(b,c) \in \mathcal{E}^{ra}$, $\beta \in \{1,\ldots,F^r_{ba}\}$ and $\gamma \in \{1,\ldots,F^{r+1}_{ca}\}$, by

$$E^{ra}(b,c)_{\beta\gamma} \;= \\ \frac{S_r^{1/2}\,\psi_c^{1/4}}{\psi_b^{1/4}} \sum_{(b,d_1,\ldots,d_{r-2},a)\,\in\,\mathcal{G}^r_{ba}} U^r(b,a)_{\beta,(b,d_1,\ldots,d_{r-2},a)}\;U^{r+1}(c,a)_{\gamma,(c,b,d_1,\ldots,d_{r-2},a)}\,. \tag{3.43}$$

We shall represent the boundary edge weights diagrammatically as

$$E^{ra}(b,c)_{\beta\gamma} \quad = \tag{3.44}$$

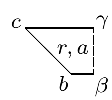

We see that

$$\text{number of } (r,a) \text{ boundary edge weights} \;=\; (F^r\,G\,F^{r+1})_{aa}\,. \tag{3.45}$$

We note, as an example, that for the $(1,a)$ boundary condition,

$$\mathcal{E}^{1a} \;=\; \{(a,c) \mid G_{ac} = 1\}\,, \quad |E^{1a}(a,c)_{11}| \;=\; (\psi_c/\psi_a)^{1/4}\,. \tag{3.46}$$

We now find, by substituting (2.29) into (3.29) and using (3.14), (3.22) and (3.23), a general expression for the boundary weights in terms of boundary edge weights,

$$B^{ra}\!\left(c\; \begin{matrix} d & \delta \\ b & \beta \end{matrix} \middle|\, u,\xi \right) \;=\; \frac{s_0(\xi-u)\; s_r(\xi+u)\; \psi_c^{1/2}}{s_0(2\xi)\; \psi_b^{1/2}}\, \delta_{bd}\, \delta_{\beta\delta} \;+\; \frac{s_0(2u)}{s_0(2\xi)} \sum_{\gamma=1}^{F_{ca}^{r+1}} E^{ra}(b,c)_{\beta\gamma}\, E^{ra}(d,c)_{\delta\gamma}\,. \tag{3.47}$$

From this, we immediately see that at $u=\xi$ the boundary weights are independent of ξ and can be decomposed as a sum of products of boundary edge weights,

$$B^{ra}\!\left(c\; \begin{matrix} d & \delta \\ b & \beta \end{matrix} \middle|\, \xi,\xi \right) = \sum_{\gamma=1}^{F_{ca}^{r+1}} E^{ra}(b,c)_{\beta\gamma}\; E^{ra}(d,c)_{\delta\gamma} \tag{3.48}$$

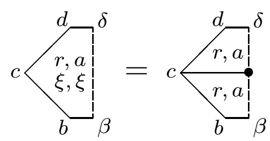

.

We note that the origin of this decomposition is the fact, apparent from (2.29), that at $u=\xi$ the boundary operators are proportional to fusion operators, so that the decomposition of boundary weights is essentially equivalent to the eigenvector decomposition of projectors.

We shall refer to this point, $u=\xi$, as the conformal point, since it is here that certain lattice models are expected to exhibit conformal behaviour, with the lattice realisation of the conformal boundary condition (r,a) being given by the set of (r,a) boundary edge weights.

We find, by using (2.30) in (3.29), that a decomposition similar to (3.48) occurs at $u=-\xi$,

$$B^{ra}\!\left(c\; \begin{matrix} d & \delta \\ b & \beta \end{matrix} \middle|\, -\xi,\xi \right) \;=\; \sum_{\substack{\gamma=1 \\ (r\neq 1)}}^{F_{ca}^{r-1}} E^{r-1,a}(c,b)_{\gamma\beta}\; E^{r-1,a}(c,d)_{\gamma\delta} \tag{3.49}$$

We therefore see that, apart from an unimportant reversal of the order of the nodes in the boundary edges, the (r,a) boundary condition at $u=-\xi$ is equivalent to the

$(r-1,a)$ boundary condition at $u=\xi$. In fact, decompositions of the form (3.48) or (3.49) also occur at other points, for example at $u=-r\lambda-\xi$, $u=r\lambda+\xi$ or points related to these by trigonometric periodicity, but since these points all involve the same boundary edge weights up to reordering of the nodes in the boundary edges or relabelling of r as $r\pm1$, we can, without loss of generality, concentrate on the single conformal point $u=\xi$.

We also note that the sum in (3.48) is empty if $F^{r+1}_{ca}=0$. It is thus possible that for a particular boundary condition, certain boundary weights are non-zero away from the conformal point but vanish at the conformal point. From (3.47), we find that such boundary weights are specifically those for which $b=d$, $\beta=\delta$, $F^r_{ba}\,G_{bc}>0$ and $F^{r+1}_{ca}=0$.

We see from (3.47) that the boundary weights satisfy the boundary anisotropy property

$$B^{ra}\!\left(c\;\begin{matrix} d & \delta \\ b & \beta \end{matrix}\,\middle|\, 0,\xi\right) \;=\; \frac{s_0(\xi)\;s_r(\xi)\;\psi_c^{1/2}}{s_0(2\xi)\;\psi_b^{1/2}}\;\delta_{bd}\;\delta_{\beta\delta}\,. \tag{3.50}$$

The second term on the right side of (3.47) also vanishes for $\xi\to\pm i\infty$ so that, assuming $\lambda/\pi\notin\mathbb{Z}$,

$$B^{ra}\!\left(c\;\begin{matrix} d & \delta \\ b & \beta \end{matrix}\,\middle|\, u,\pm i\infty\right) \;=\; \pm\,\frac{i\;e^{\mp ir\lambda}\;\psi_c^{1/2}}{2\;\sin\lambda\;\psi_b^{1/2}}\;\;\delta_{bd}\;\delta_{\beta\delta}\,. \tag{3.51}$$

Comparing the right sides of (3.50) or (3.51) with the $(1,a)$ boundary weights (3.32), we see that at $u=0$ or $\xi\to\pm i\infty$ the nonzero (r,a) boundary weights reduce, up to unimportant normalisation, to $(1,b)$ boundary weights, with each $(1,b)$ weight for any b appearing F^r_{ab} (which may be zero) times.

Finally, we note that a gauge transformation of the boundary edge weights,

$$E^{ra}(b,c)_{\beta\gamma}\;\mapsto\;\sum_{\beta'=1}^{F^r_{ba}}\;\sum_{\gamma'=1}^{F^{r+1}_{ca}}\;S^{ra}(b)_{\beta\beta'}\;S^{r+1,a}(c)_{\gamma\gamma'}\;E^{ra}(b,c)_{\beta'\gamma'}\,, \tag{3.52}$$

induces a gauge transformation (3.36) of the boundary weights, for any $S^{ra}(e)$ satisfying (3.37).

3.7 Transfer Matrices and the Partition Function

We now proceed to a study of some aspects of the complete lattice. We shall be considering a square lattice on a cylinder of width N and circumference $2M$ lattice spacings, with the left boundary condition and boundary field given by (r_1, a_1) and ξ_1 and the right boundary condition and boundary field given by (r_2, a_2) and ξ_2. In particular, we shall express the partition function for the model using double-row transfer matrices, these being defined in terms of the bulk and boundary weights of the previous sections. Double-row transfer matrices of this type were introduced in [2] and first used for interaction-round-a-face models in [31].

An additional feature of the lattice to be considered here is that alternate rows will be associated with spectral parameter values u and λ–u. Also, the left boundary will be associated with the spectral parameter value $\lambda-u$ while the right boundary will be associated with the value u. These spectral parameter values are used since they result in the double-row transfer matrices forming a commuting family. The most physically relevant point is the isotropic point $u = \lambda/2$, at which all rows and both boundaries are associated with the same value of the spectral parameter. Combining this with the conformal point described in the previous section, the case of most interest here is thus $u = \xi_1 = \xi_2 = \lambda/2$.

We begin by defining a set of paths consistent with boundary conditions (r_1, a_1) and (r_2, a_2) and lattice width N,

$$\begin{aligned}\mathcal{G}^{N}_{r_1a_1|r_2a_2} \;=\; \Big\{(\beta_1, b_0, \ldots, b_{N}, \beta_2)\,\Big|\,(b_0, \ldots, b_{N}) \in \mathcal{G}^{N+1},\ F^{r_1}_{a_1b_0}F^{r_2}_{b_Na_2} > 0,\\ \beta_1 \in \{1, \ldots, F^{r_1}_{a_1b_0}\},\ \beta_2 \in \{1, \ldots, F^{r_2}_{b_Na_2}\}\Big\}\,.\end{aligned} \tag{3.53}$$

We see that

$$|\mathcal{G}^{N}_{r_1a_1|r_2a_2}| \;=\; (F^{r_1}\,G^{N}F^{r_2})_{a_1a_2}\,, \tag{3.54}$$

which is invariant under interchange of a_1 and a_2 or r_1 and r_2, since F^{r_1}, F^{r_2} and G are symmetric and mutually commuting matrices.

We now introduce a double-row transfer matrix $\boldsymbol{D}^{N}_{r_1a_1|r_2a_2}(u, \xi_1, \xi_2)$ with rows and columns labelled by the paths of $\mathcal{G}^N_{r_1a_1|r_2a_2}$ and entries defined by

$$
\begin{aligned}
&\boldsymbol{D}^N_{r_1a_1|r_2a_2}(u,\xi_1,\xi_2)_{(\beta_1,b_0,\ldots,b_N,\beta_2),(\delta_1,d_0,\ldots,d_N,\delta_2)} \;=\\
&\qquad\sum_{\substack{(c_0,\ldots,c_N)\,\in\,\mathcal{G}^{N+1}\\ (\prod_{j=0}^{N} G_{b_jc_j}G_{c_jd_j}=1)}} B^{r_1a_1}\!\left(c_0\;\begin{matrix} d_0 & \delta_1\\ b_0 & \beta_1\end{matrix}\;\middle|\;\lambda-u,\xi_1\right)\;\times\\
&\qquad\quad\left[\prod_{j=0}^{N-1} W\!\left(\begin{matrix} c_j & c_{j+1}\\ b_j & b_{j+1}\end{matrix}\;\middle|\;u\right) W\!\left(\begin{matrix} d_j & d_{j+1}\\ c_j & c_{j+1}\end{matrix}\;\middle|\;\lambda-u\right)\right] B^{r_2a_2}\!\left(c_N\;\begin{matrix} d_N & \delta_2\\ b_N & \beta_2\end{matrix}\;\middle|\;u,\xi_2\right) \qquad (3.55)
\end{aligned}
$$

$=$ 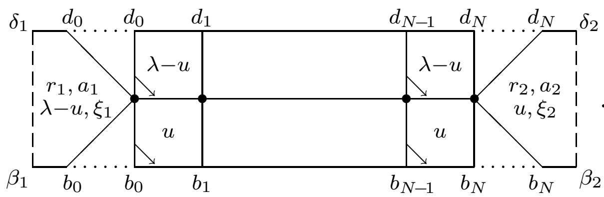

.

We note that if $\mathcal{G}^N_{r_1a_1|r_2a_2}$ is empty, then $\boldsymbol{D}^N_{r_1a_1|r_2a_2}(u,\xi_1,\xi_2)$ is zero-dimensional with its value taken as 0.

The partition function for the lattice model is now given by

$$\boldsymbol{Z}^{NM}_{r_1a_1|r_2a_2}(u,\xi_1,\xi_2) \;=\; \mathrm{tr}\,\big(\boldsymbol{D}^N_{r_1a_1|r_2a_2}(u,\xi_1,\xi_2)\big)^M$$

$=$ 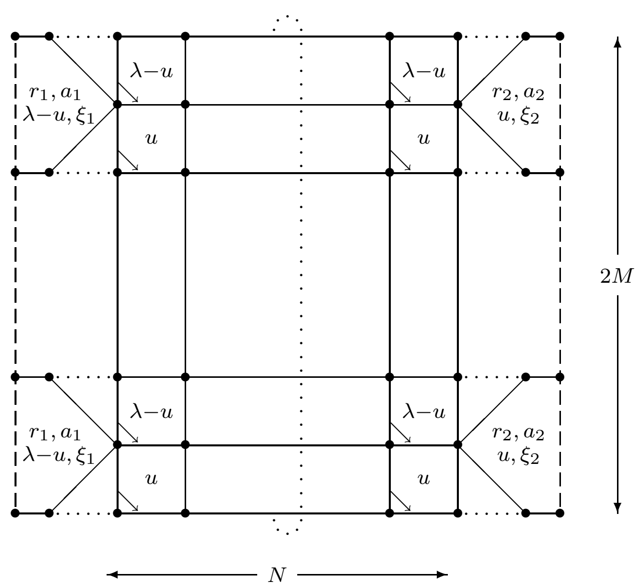

. (3.56)

We can see from the first equality that the task of evaluating the partition function is equivalent to that of evaluating the eigenvalues $\Lambda^N_{r_1a_1|r_2a_2}(u,\xi_1,\xi_2)_k$, where $k = 1,\ldots,(F^{r_1}G^NF^{r_2})_{a_1a_2}$, of the double-row transfer matrix $\boldsymbol{D}^N_{r_1a_1|r_2a_2}(u,\xi_1,\xi_2)$, with

$$\boldsymbol{Z}^{NM}_{r_1a_1|r_2a_2}(u,\xi_1,\xi_2) \;=\; \sum_k \left(\Lambda^N_{r_1a_1|r_2a_2}(u,\xi_1,\xi_2)_k\right)^M . \tag{3.57}$$

3.8 Transfer Matrix Properties

We now consider a variety of properties of the double-row transfer matrices, each of which implies corresponding properties for the transfer matrix eigenvalues and hence for the partition function. In particular, we shall find that applying certain transformations to the parameters of the model results only in similarity transformations of the transfer matrix. This implies that these parameter transformations are symmetries of the model, since the transfer matrix eigenvalues and partition function are invariant under any similarity transformation of the transfer matrix.

3.8.1 Commutation

It follows from the Yang-Baxter equation (3.12), inversion relation (3.13), and boundary Yang-Baxter equation (3.34) that the double-row transfer matrices commute for any two values, u and v, of the spectral parameter,

$$\Big[\boldsymbol{D}^N_{r_1a_1|r_2a_2}(u,\xi_1,\xi_2)\;,\;\boldsymbol{D}^N_{r_1a_1|r_2a_2}(v,\xi_1,\xi_2)\Big] \;=\; 0\,. \tag{3.58}$$

This can be proved diagrammatically, as done in Section 3.4 of [31].

3.8.2 Transposition

It follows straightforwardly from (3.10) and (3.39) that each double-row transfer matrix is similar to a symmetric matrix. More specifically, defining

$$\boldsymbol{A}^N_{r_1a_1|r_2a_2\;(\beta_1,b_0,\ldots,b_N,\beta_2),(\delta_1,d_0,\ldots,d_N,\delta_2)} \;=\; \frac{\psi_{b_N}^{1/4}}{\psi_{b_0}^{1/4}}\;\delta_{(\beta_1,b_0,\ldots,b_N,\beta_2),(\delta_1,d_0,\ldots,d_N,\delta_2)} \tag{3.59}$$

and

$$\tilde{\boldsymbol{D}}^N_{r_1a_1|r_2a_2}(u,\xi_1,\xi_2) \;=\; \boldsymbol{A}^N_{r_1a_1|r_2a_2}\;\boldsymbol{D}^N_{r_1a_1|r_2a_2}(u,\xi_1,\xi_2)\;(\boldsymbol{A}^N_{r_1a_1|r_2a_2})^{-1}\,, \tag{3.60}$$

we have

$$\left(\tilde{\boldsymbol{D}}^{N}_{r_1a_1|r_2a_2}(u,\xi_1,\xi_2)\right)^T \;=\; \tilde{\boldsymbol{D}}^{N}_{r_1a_1|r_2a_2}(u,\xi_1,\xi_2)\,. \tag{3.61}$$

This implies that if u, ξ_1 and ξ_2 are taken so that the entries of $\boldsymbol{D}^{N}_{r_1a_1|r_2a_2}(u,\xi_1,\xi_2)$ are real, which since $\cos\lambda$ is real is always possible, then $\boldsymbol{D}^{N}_{r_1a_1|r_2a_2}(u,\xi_1,\xi_2)$ is completely diagonalisable and each of its eigenvalues is real. Furthermore, due to the commutation (3.58), there exists a simultaneous set of eigenvectors for all values of the spectral parameter. That is, there exists a basis of u-independent eigenvectors, which has the important consequence that u-dependent equations satisfied by the transfer matrix are also satisfied by each of its eigenvalues. It is essentially for these reasons that the model is regarded as being integrable.

3.8.3 Gauge Invariance

We see that the model is invariant under any gauge transformation (3.36) of the boundary weights since this results only in a similarity transformation of the double-row transfer matrix,

$$\boldsymbol{D}^{N}_{r_1a_1|r_2a_2}(u,\xi_1,\xi_2) \;\mapsto\; \boldsymbol{S}^{N}_{r_1a_1|r_2a_2}\;\boldsymbol{D}^{N}_{r_1a_1|r_2a_2}(u,\xi_1,\xi_2)\;(\boldsymbol{S}^{N}_{r_1a_1|r_2a_2})^{-1}\,, \tag{3.62}$$

where

$$\begin{aligned}\boldsymbol{S}^{N}_{r_1a_1|r_2a_2\;(\beta_1,b_0,\ldots,b_N,\beta_2),(\delta_1,d_0,\ldots,d_N,\delta_2)} \;&=\\ &S^{r_1a_1}(b_0)_{\beta_1\delta_1}\;S^{r_2a_2}(b_N)_{\beta_2\delta_2}\;\delta_{(b_0,\ldots,b_N),(d_0,\ldots,d_N)}\,.\end{aligned} \tag{3.63}$$

3.8.4 Simplification at Completely Anisotropic Points

It follows from the anisotropy property (3.11), boundary anisotropy property (3.50), crossing symmetry (3.10) and boundary crossing symmetry (3.40) that at the completely anisotropic points, $u=0$ and $u=\lambda$, the double-row transfer matrices are proportional to the identity,

$$\boldsymbol{D}^{N}_{r_1a_1|r_2a_2}(0,\xi_1,\xi_2) \;=\; \boldsymbol{D}^{N}_{r_1a_1|r_2a_2}(\lambda,\xi_1,\xi_2) \;=\; \frac{S_2\,s_0(\xi_1)\,s_0(\xi_2)\,s_{r_1}(\xi_1)\,s_{r_2}(\xi_2)}{s_0(2\xi_1)\,s_0(2\xi_2)}\,\boldsymbol{I}\,. \tag{3.64}$$

3.8.5 Crossing Symmetry

It follows from the Yang-Baxter equation (3.12), inversion relation (3.13) and boundary crossing symmetry (3.40) that the double-row transfer matrices satisfy crossing symmetry,

$$\boldsymbol{D}^N_{r_1a_1|r_2a_2}(\lambda - u, \xi_1, \xi_2) \;=\; \boldsymbol{D}^N_{r_1a_1|r_2a_2}(u, \xi_1, \xi_2)\,. \tag{3.65}$$

This, like (3.58), can be proved diagrammatically, as done in Section 3.3 of [31].

3.8.6 Left-Right Symmetry

It follows from reflection symmetry (3.9) and boundary reflection symmetry (3.39) that on interchanging the left and right boundary conditions and boundary fields, we have

$$\boldsymbol{D}^N_{r_2a_2|r_1a_1}(u, \xi_2, \xi_1)\; \boldsymbol{R}^N_{r_1a_1|r_2a_2} \;=\; \boldsymbol{R}^N_{r_1a_1|r_2a_2}\, \Big(\boldsymbol{D}^N_{r_1a_1|r_2a_2}(\lambda - u, \xi_1, \xi_2)\Big)^T, \tag{3.66}$$

where $\boldsymbol{R}^N_{r_1a_1|r_2a_2}$ is a square matrix with rows labelled by the paths of $\mathcal{G}^N_{r_2a_2|r_1a_1}$, columns labelled by the paths of $\mathcal{G}^N_{r_1a_1|r_2a_2}$ and entries given by

$$\boldsymbol{R}^N_{r_1a_1|r_2a_2\;(\beta_1,b_0,\ldots,b_N,\beta_2),(\delta_1,d_0,\ldots,d_N,\delta_2)} \;=\; \delta_{(\beta_2,b_N,\ldots,b_0,\beta_1),(\delta_1,d_0,\ldots,d_N,\delta_2)}\,. \tag{3.67}$$

Combining (3.66) and the invertibility of $\boldsymbol{R}^N_{r_1a_1|r_2a_2}$ with (3.61) and (3.65), we see that $\boldsymbol{D}^N_{r_1a_1|r_2a_2}(u, \xi_1, \xi_2)$ and $\boldsymbol{D}^N_{r_2a_2|r_1a_1}(u, \xi_2, \xi_1)$ are related by a similarity transformation, so that this complete interchanging of the left and right boundaries is a symmetry of the model.

3.8.7 Symmetry under Interchange of r_1, ξ_1 and r_2, ξ_2

It can also be shown that under interchange of r_1, ξ_1 and r_2, ξ_2, we have

$$\boldsymbol{D}^N_{r_2a_1|r_1a_2}(u, \xi_2, \xi_1)\; \boldsymbol{C}^N_{r_1a_1|r_2a_2}(\xi_1, \xi_2) \;=\; \boldsymbol{C}^N_{r_1a_1|r_2a_2}(\xi_1, \xi_2)\; \boldsymbol{D}^N_{r_1a_1|r_2a_2}(u, \xi_1, \xi_2)\,, \tag{3.68}$$

where $\boldsymbol{C}^N_{r_1a_1|r_2a_2}(\xi_1,\xi_2)$ is a square matrix with rows labelled by the paths of $\mathcal{G}^N_{r_2a_1|r_1a_2}$, columns labelled by the paths of $\mathcal{G}^N_{r_1a_1|r_2a_2}$ and entries given by

$$\begin{aligned}\boldsymbol{C}^N_{r_1a_1|r_2a_2}(\xi_1,\xi_2)_{(\beta_1,b_0,\ldots,b_N,\beta_2),(\delta_1,d_0,\ldots,d_N,\delta_2)} \;&=\; \frac{(\psi_{b_0}\,\psi_{b_N}\,\psi_{d_0}\,\psi_{d_N})^{1/4}}{(\psi_{a_1}\,\psi_{a_2})^{1/2}}\times\\ &\sum_{\substack{(c_0,\ldots,c_{N-1})\,\in\,\mathcal{G}^N\\ (G_{c_{N-1}a_2}\prod_{j=0}^{N-1}F^{r_1}_{b_jc_j}F^{r_2}_{c_jd_j}>0)}}\;\sum_{\alpha_0=1}^{F^{r_1}_{b_0c_0}}\cdots\sum_{\alpha_{N-1}=1}^{F^{r_1}_{b_{N-1}c_{N-1}}}\;\sum_{\gamma_0=1}^{F^{r_2}_{c_0d_0}}\cdots\sum_{\gamma_{N-1}=1}^{F^{r_2}_{c_{N-1}d_{N-1}}} W^{r_2r_1}\!\left(\begin{matrix}d_0&\gamma_0&c_0\\ \delta_1&&\alpha_0\\ a_1&\beta_1&b_0\end{matrix}\;\middle|\;\begin{matrix}\xi_1-\xi_2\\ +\lambda\end{matrix}\right)\\ &\times\left[\prod_{j=0}^{N-1}W^{2r_1}\!\left(\begin{matrix}c_j&1&c_{j+1}\\ \alpha_j&&\alpha_{j+1}\\ b_j&1&b_{j+1}\end{matrix}\;\middle|\;\xi_1+2\lambda\right)\,W^{2r_2}\!\left(\begin{matrix}d_j&1&d_{j+1}\\ \gamma_j&&\gamma_{j+1}\\ c_j&1&c_{j+1}\end{matrix}\;\middle|\;\xi_2+\lambda\right)\right],\end{aligned}\tag{3.69}$$

in which we take $c_N=a_2$, $\alpha_N=\beta_2$ and $\gamma_N=\delta_2$.

The weights which appear in (3.69) are fused bulk weights which are defined, for each $r,s\in\{1,\ldots,g-1\}$, as fused $r-1$ by $s-1$ blocks of bulk weights,

$$W^{rs}\!\left(\begin{matrix}d&\gamma&c\\ \delta&&\beta\\ a&\alpha&b\end{matrix}\;\middle|\;u\right)\;=\tag{3.70}$$

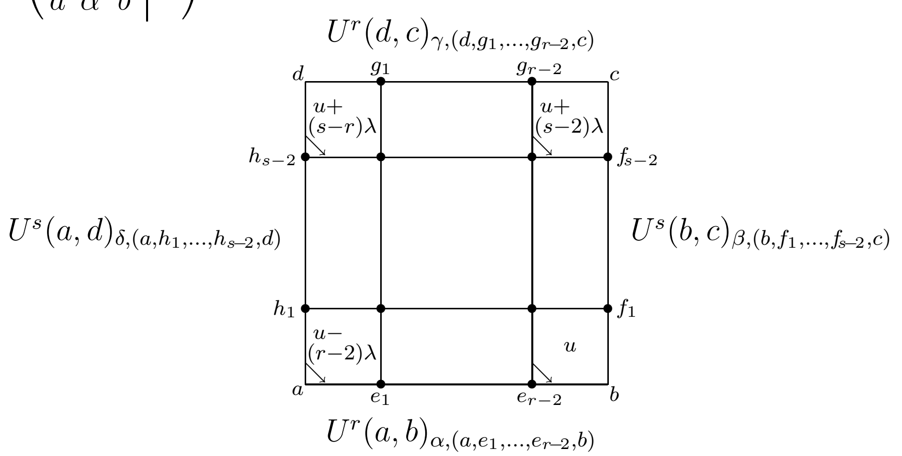

These fused weights can be regarded as lattice generalisations of the 1 by $r-1$ and $r-1$ by 1 fused blocks considered in (2.20). They satisfy a generalised Yang-Baxter equation, as given in (3.39) of [42], and it is by using this equation, and expressing the boundary weights in the double row transfer matrices in the form (3.33), that

(3.68) can be proved. In doing this, it is the $(\xi_1+2\lambda)$-dependent 1 by r_1-1 fused weights in (3.69) which, together with the generalised Yang-Baxter equation, allow the ξ_1-dependent r_1-1 by 2 fused block of bulk weights within the left boundary weight to be propagated to the right. Similarly, it is the $(\xi_2+\lambda)$-dependent 1 by r_2-1 fused weights which allow the ξ_2-dependent r_2-1 by 2 fused block within the right boundary weight to be propagated to the left, and it is the $(\xi_1-\xi_2+\lambda)$-dependent r_2-1 by r_1-1 fused weight which allows the two blocks of bulk weights from the left and right boundary weights to be interchanged.

We also note that the generalised Yang-Baxter equation allows the fused weights within $\boldsymbol{C}^N_{r_1a_1|r_2a_2}(\xi_1,\xi_2)$ to be rearranged. In particular, the $(\xi_1-\xi_2+\lambda)$-dependent fused weight, which in (3.69) is on the far left of the lattice row, can be propagated to an arbitrary position further to the right, while reversing the order of the $(\xi_1+2\lambda)$- and $(\xi_2+\lambda)$-dependent fused weights to the left of it final position. This essentially corresponds to the fact that, in proving (3.68), the order with which the blocks from the left and right boundaries are interchanged is arbitrary.

By using a generalised inversion relation, it can also be shown that $\boldsymbol{C}^N_{r_1a_1|r_2a_2}(\xi_1,\xi_2)$ is invertible (except at isolated values of ξ_1 or ξ_2, which by continuity are unimportant), its inverse being proportional to $\boldsymbol{C}^N_{r_2a_1|r_1a_2}(\xi_2,\xi_1)$. It thus follows that transfer matrices with r_1, ξ_1 and r_2, ξ_2 interchanged are related by a similarity transformation, so that this partial interchanging of the left and right boundaries is a symmetry of the model.

Finally, we note that a simple generalisation of the results of this section is that it is also possible, up to similarity transformation, to propagate the fused block of bulk weights within either boundary weight to an arbitrary position within the interior of the transfer matrix. The importance of this observation is that it is consistent with the viewpoint in conformal field theory of the boundary conditions corresponding to local operators.

3.8.8 Properties Arising from $\xi\to i\infty$

Various properties follow from the $\xi\to i\infty$ (or equivalently $\xi\to -i\infty$) form (3.51) of the boundary weights.

For example, applying this limit to both the left and right boundary fields we find that $\boldsymbol{D}^N_{r_1a_1|r_2a_2}(u,i\infty,i\infty)$ is proportional to a direct sum, over $a_1{}',a_2{}'\in\mathcal{G}$, of $\boldsymbol{D}^N_{1a_1{}'|1a_2{}'}(u,\xi_1,\xi_2)$, with this term being repeated $F^{r_1}_{a_1a_1{}'}F^{r_2}_{a_2a_2{}'}$ times in the sum.

As a further example, we can attach an additional $r_1{}'$ by 2 fused block on the left and an additional $r_2{}'$ by 2 fused block on the right of $\boldsymbol{D}^N_{r_1a_1|r_2a_2}(u,\xi_1,\xi_2)$, where each of these blocks is of the same form as that in (3.33) and we take $\xi\to i\infty$ in each. We then find, from (3.51), that the resulting matrix is proportional to a corresponding direct sum and, using methods similar to those of Section 3.8.7, that the two attached blocks can be interchanged up to similarity transformation. This therefore gives the result

$$\bigoplus_{a_1{}',a_2{}'\in\mathcal{G}}^{F^{r_1}_{a_1a_1{}'}F^{r_2}_{a_2a_2{}'}} \boldsymbol{D}^N_{r_1{}'a_1{}'|r_2{}'a_2{}'}(u,\xi_1,\xi_2) \;\approx\; \bigoplus_{a_1{}',a_2{}'\in\mathcal{G}}^{F^{r_2}_{a_1a_1{}'}F^{r_1}_{a_2a_2{}'}} \boldsymbol{D}^N_{r_1{}'a_1{}'|r_2{}'a_2{}'}(u,\xi_1,\xi_2)\,, \tag{3.71}$$

where $\approx$ indicates equality up to similarity transformation and the superscripts on $\bigoplus$ indicate the number of times that the corresponding terms appear in the direct sum. This relation implies that

$$\sum_{a_1{}',a_2{}'\in\mathcal{G}} F^{r_1}_{a_1a_1{}'}\,F^{r_2}_{a_2a_2{}'}\,\boldsymbol{Z}^{NM}_{r_1{}'a_1{}'|r_2{}'a_2{}'}(u,\xi_1,\xi_2) \;=\; \sum_{a_1{}',a_2{}'\in\mathcal{G}} F^{r_2}_{a_1a_1{}'}\,F^{r_1}_{a_2a_2{}'}\,\boldsymbol{Z}^{NM}_{r_1{}'a_1{}'|r_2{}'a_2{}'}(u,\xi_1,\xi_2)\,. \tag{3.72}$$

3.8.9 Decomposition into Single-Row Transfer Matrices at the Conformal Point

It follows from (3.48) that if both boundaries are at their conformal point, that is if $u=\lambda-\xi_1=\xi_2\equiv\xi$, then the double-row transfer matrix decomposes into a product of two single-row transfer matrices. We denote these, generally not square, matrices as $\check{\boldsymbol{T}}^N_{r_1a_1|r_2a_2}(\xi)$, with rows labelled by the paths of $\mathcal{G}^N_{r_1a_1|r_2a_2}$ and columns labelled by the paths of $\mathcal{G}^N_{r_1+1,a_1|r_2+1,a_2}$, and $\hat{\boldsymbol{T}}^N_{r_1a_1|r_2a_2}(\xi)$, with rows labelled by the paths of $\mathcal{G}^N_{r_1+1,a_1|r_2+1,a_2}$ and columns labelled by the paths of $\mathcal{G}^N_{r_1a_1|r_2a_2}$. The entries of these matrices are given by

$$\overset{\vee}{\boldsymbol{T}}{}^{N}_{r_1a_1|r_2a_2}(\xi)_{(\beta_1,b_0,\ldots,b_N,\beta_2),(\gamma_1,c_0,\ldots,c_N,\gamma_2)} \;=\; \begin{cases} E^{r_1a_1}(b_0,c_0)_{\beta_1\gamma_1}\displaystyle\prod_{j=0}^{N-1} W\!\left(\begin{matrix} c_j & c_{j+1} \\ b_j & b_{j+1}\end{matrix}\,\middle|\, \xi\right) E^{r_2a_2}(b_N,c_N)_{\beta_2\gamma_2}, & \displaystyle\prod_{j=0}^{N} G_{b_jc_j}=1 \\[2ex] 0\,, \quad \displaystyle\prod_{j=0}^{N} G_{b_jc_j}=0 \end{cases} \tag{3.73}$$

$=$ 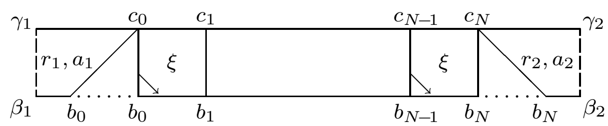

and

$$\overset{\wedge}{\boldsymbol{T}}{}^{N}_{r_1a_1|r_2a_2}(\xi)_{(\gamma_1,c_0,\ldots,c_N,\gamma_2),(\beta_1,b_0,\ldots,b_N,\beta_2)} \;=\; \begin{cases} E^{r_1a_1}(b_0,c_0)_{\beta_1\gamma_1}\displaystyle\prod_{j=0}^{N-1} W\!\left(\begin{matrix} b_j & b_{j+1} \\ c_j & c_{j+1}\end{matrix}\,\middle|\, \lambda-\xi\right) E^{r_2a_2}(b_N,c_N)_{\beta_2\gamma_2}, & \displaystyle\prod_{j=0}^{N} G_{c_jb_j}=1 \\[2ex] 0\,, \quad \displaystyle\prod_{j=0}^{N} G_{c_jb_j}=0 \end{cases} \tag{3.74}$$

$=$ 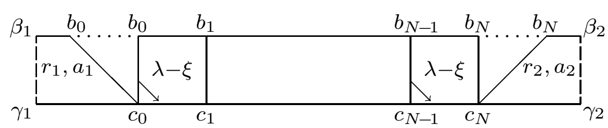 .

We now see, using (3.48), that the decomposition of the double-row transfer matrix at the conformal point is

$$\boldsymbol{D}^{N}_{r_1a_1|r_2a_2}(\xi,\lambda-\xi,\xi) \;=\; \overset{\vee}{\boldsymbol{T}}{}^{N}_{r_1a_1|r_2a_2}(\xi)\;\; \overset{\wedge}{\boldsymbol{T}}{}^{N}_{r_1a_1|r_2a_2}(\xi)\,. \tag{3.75}$$

We emphasise that the orientations of the boundary edge weights in the two single-row transfer matrices in (3.75) are opposite with respect to a fixed direction along the boundary. Thus, even at the isotropic point $\xi = \lambda/2$, at which adjacent rows of the lattice become indistinguishable in the bulk, the alternating orientations of the boundary edge weights will still distinguish adjacent rows at the boundaries.

We see from (3.10) that $\overset{\wedge}{\boldsymbol{T}}{}^N_{r_1a_1|r_2a_2}(\xi) = (\boldsymbol{A}^N_{r_1+1,a_1|r_2+1,a_2})^{-2}(\overset{\vee}{\boldsymbol{T}}{}^N_{r_1a_1|r_2a_2}(\xi))^T(\boldsymbol{A}^N_{r_1a_1|r_2a_2})^2$, where $\boldsymbol{A}^N_{r_1a_1|r_2a_2}$ is given by (3.59), and therefore that

$$\boldsymbol{D}^N_{r_1a_1|r_2a_2}(\xi,\lambda-\xi,\xi) \;=\; (\boldsymbol{A}^N_{r_1a_1|r_2a_2})^{-1}\,\tilde{\boldsymbol{T}}^N_{r_1a_1|r_2a_2}(\xi)\,\Big(\tilde{\boldsymbol{T}}^N_{r_1a_1|r_2a_2}(\xi)\Big)^T\,\boldsymbol{A}^N_{r_1a_1|r_2a_2}\,, \tag{3.76}$$

where $\tilde{\boldsymbol{T}}^N_{r_1a_1|r_2a_2}(\xi) \;=\; \boldsymbol{A}^N_{r_1a_1|r_2a_2}\;\overset{\vee}{\boldsymbol{T}}{}^N_{r_1a_1|r_2a_2}(\xi)(\boldsymbol{A}^N_{r_1a_1|r_2a_2})^{-1}$. This immediately implies that if ξ is taken so that the entries of $\boldsymbol{D}^N_{r_1a_1|r_2a_2}(\xi,\lambda-\xi,\xi)$ are real, then the eigenvalues of this matrix are all nonnegative.

3.8.10 Properties Arising from Graph Bicolourability

We now consider some properties which arise if the graph $\mathcal{G}$ is bicolourable. Although we have not assumed until now that $\mathcal{G}$ is bicolourable, all of the specific A, D and E cases to be considered in the next section have this property.

Bicolourability of $\mathcal{G}$ means that a parity $\pi_a \in \{-1,1\}$ can be assigned to each node $a \in \mathcal{G}$ so that adjacent nodes always have opposite parity; that is,

$$G_{ab} = 1 \implies \pi_a\,\pi_b = -1\,. \tag{3.77}$$

We now note that it follows from (3.18) that each F^r with r even/odd is an odd/even polynomial in G, which leads to a generalisation of (3.77) to a selection rule on the fused adjacency matrices,

$$F^r_{ab} > 0 \implies \pi_a\,\pi_b = (-1)^{r+1}\,. \tag{3.78}$$

Proceeding to the effect of graph bicolourability on the lattice model, a square lattice can be naturally divided into two interpenetrating sublattices, with the nearest neighbours of each site on one sublattice being sites on the other. Thus, if $\mathcal{G}$ is bicolourable then the condition that the spin states on neighbouring lattice sites be adjacent nodes on $\mathcal{G}$ implies that, in each spin assignment, the spin states on one sublattice all have parity 1, while those on the other all have parity -1.

Using (3.78), there is also a consistency condition between the left and right boundary conditions,

$$\pi_{a_1}\,\pi_{a_2} \;=\; (-1)^{r_1+r_2+N}\,, \tag{3.79}$$

since otherwise $\mathcal{G}^N_{r_1a_1|r_2a_2}$ is empty and $\boldsymbol{D}^N_{r_1a_1|r_2a_2}(u,\xi_1,\xi_2)$ and $\boldsymbol{Z}^{NM}_{r_1a_1|r_2a_2}(u,\xi_1,\xi_2)$ are zero. If this condition is satisfied, then the sublattices are fixed by the boundary conditions; that is, the sublattice which contains all parity 1, or all parity -1, spin states is the same for all possible assignments.

Finally, we note that (3.78) also implies that for each boundary edge $(b,c)\in\mathcal{E}^{ra}$, the parities of b and c are respectively opposite to and the same as $\pi_a\,(-1)^r$, and that therefore any pair of nodes can appear in only one order in a particular set of boundary edges.

4. *A–D–E* Models

We now specialise to models whose graph $\mathcal{G}$ is an A, D or E Dynkin diagram with Coxeter number g. In these cases, λ is real and the regime of interest here is $0<u<\lambda$. This class of models was first identified and studied in [8]. The A and D models are the critical limits of models introduced in [45] and [46] respectively, but the E models do not have off-critical counterparts.

Fusion of the A models was introduced in [39, 40, 41], while fusion of the D and E models was first studied in [42]. We shall also consider intertwiner relations among these models, these having been studied in detail in [21, 47, 48, 49]. In particular, we shall find that certain symmetries in the fusion and intertwiner properties of these models lead to various additional properties of the boundary conditions, transfer matrices and partition functions.

We shall also study the explicit forms of the boundary weights and boundary edge weights for these models. For the A models, various methods have previously been used to obtain sets of diagonal boundary weights in [4, 30, 31, 32] and sets containing non-diagonal weights in [4, 29, 30, 32, 33], and all of the A boundary weights found here represent certain cases of these previously-known weights. For the D and E models, sets of diagonal boundary weights were found by direct solution of the boundary Yang-Baxter equation in [32], but most of the sets obtained here contain non-diagonal weights and were not previously known.

Finally, we shall consider the connection between the lattice model boundary conditions at the conformal and isotropic points and the conformal boundary conditions of the corresponding unitary minimal theories.

4.1 Graphs and Adjacency Matrices

The A, D and E Dynkin diagrams with Coxeter number g are explicitly given by

$A_{g-1} \;=$ 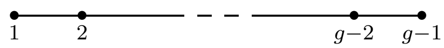

$, \qquad g \;=\; 2, 3, \dots\,, \qquad (4.1)$

$D_{\frac{g}{2}+1} \;=$ 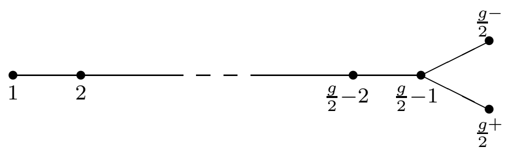

$, \qquad g \;=\; 6, 8, \dots\,, \qquad (4.2)$

$E_6 \;=$ 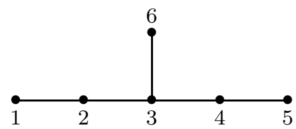

$, \qquad g \;=\; 12\,, \qquad (4.3)$

$E_7 \;=$ 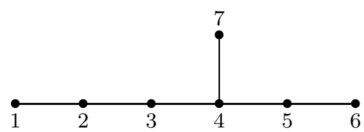

$, \qquad g \;=\; 18\,, \qquad (4.4)$

and

$E_8 \;=$ 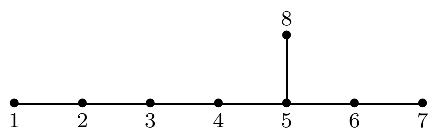

$, \qquad g \;=\; 30\,. \qquad (4.5)$

We note that when referring to the nodes $\frac{g}{2}^-$ and $\frac{g}{2}^+$ of $D_{\frac{g}{2}+1}$, we shall use the convention that if the superscript is not specified then the choice is immaterial. Furthermore, if a numerical value for $\frac{g}{2}^-$ or $\frac{g}{2}^+$ is required in any equation, it is to be taken as $\frac{g}{2}$.

For each of these graphs, we set

$$\lambda = \pi/g\,, \tag{4.6}$$

from which we see that g matches that defined in (2.11), and for which $2\cos\lambda$ is known to be the largest eigenvalue of the adjacency matrix as required. The entries of the corresponding Perron-Frobenius eigenvectors are then given by

$$\psi_a \;=\; \begin{cases} S_a\,, \quad a=1,\ldots,g{-}1\;; & A_{g-1} \\[4pt] \begin{cases} S_a\,, & a=1,\ldots,\frac{g}{2}-1 \\ 1\,/\,(2\sin\lambda)\,, & a=\frac{g}{2} \end{cases} \;; & D_{\frac{g}{2}+1} \\[4pt] \begin{cases} S_a\,, & a=1,\ldots,l{-}3 \\ \sin(l{-}1)\lambda\,/\,\sin 2\lambda\,, & a=l{-}2 \\ 2\cos(l{-}2)\lambda\,, & a=l{-}1 \\ \sin(l{-}3)\lambda\,/\,\sin 2\lambda\,, & a=l \end{cases} \;; & E_l\,,\; l=6,7,8\,, \end{cases} \tag{4.7}$$

where, from (2.4), $S_a = \sin a\lambda\,/\,\sin\lambda$.

It is also important here to consider a particular involution $a \mapsto \bar{a}$ of the nodes of each graph, this being given by the graph's $\mathbb{Z}_2$ symmetry transformation for the A, $D_{\rm odd}$ and E_6 cases and by the identity for the $D_{\rm even}$, E_7 and E_8 cases. More explicitly, we have

$$\bar{a} \;=\; \begin{cases} g{-}a\,, & a \in A_{g-1} \\ \frac{g}{2}^{\mp}\,, & a=\frac{g}{2}^{\pm} \in D_{\frac{g}{2}+1}\,, \quad \frac{g}{2}{+}1 \text{ odd} \\ 6{-}a\,, & a \in E_6/\{6\} \\ a\,, & \text{otherwise}\,. \end{cases} \tag{4.8}$$

We see that the eigenvector entries (4.7) are invariant under this involution,

$$\psi_{\bar{a}} = \psi_a\,. \tag{4.9}$$

We also observe that each A, D and E graph is bicolourable and that we may set the parities as

$$\pi_a \;=\; (-1)^a\,. \tag{4.10}$$

We now consider the A, D and E fused adjacency matrices. A more comprehensive treatment of these can be found in Appendix B of [7].

For A_{g-1}, we have explicitly

$$F^r_{ab} \;=\; \begin{cases} 1\,; & a{+}b{+}r \text{ odd}, \;\; |a-b| \le r{-}1 \;\text{ and }\; r{+}1 \le a+b \le 2g{-}r{-}1 \\ 0\,; & \text{otherwise}\,. \end{cases} \tag{4.11}$$

We note that F^r_{ab} for A_{g-1}, with $r \neq g$, is actually symmetric in all three indices.

For $D_{\frac{g}{2}+1}$, we have explicitly

$$F^r_{ab} \;=\; \begin{cases} 2\,; & a,b \neq \frac{g}{2},\;\; a{+}b{+}r \text{ odd},\;\; |a-b| \leq \frac{g}{2}{-}|\frac{g}{2}{-}r|{-}1 \\ & \qquad \text{and}\;\; a{+}b{-}\frac{g}{2} \geq |\frac{g}{2}{-}r|{+}1 \\ 1\,; & a,b \neq \frac{g}{2},\;\; a{+}b{+}r \text{ odd},\;\; |a-b| \leq \frac{g}{2}{-}|\frac{g}{2}{-}r|{-}1 \\ & \qquad \text{and}\;\; |a{+}b{-}\frac{g}{2}| \leq |\frac{g}{2}{-}r|{-}1 \\ 1\,; & a \neq \frac{g}{2},\;\; b = \frac{g}{2},\;\; a{+}\frac{g}{2}{+}r \text{ odd}\;\; \text{and}\;\; a \geq |\frac{g}{2}{-}r|{+}1 \\ 1\,; & a = \frac{g}{2},\;\; b \neq \frac{g}{2},\;\; b{+}\frac{g}{2}{+}r \text{ odd}\;\; \text{and}\;\; b \geq |\frac{g}{2}{-}r|{+}1 \\ 1\,; & a = \frac{g}{2}^{\pm},\;\; b = \frac{g}{2}^{\pm}\;\; \text{and}\;\; r \equiv 1 \bmod 4 \\ 1\,; & a = \frac{g}{2}^{\pm},\;\; b = \frac{g}{2}^{\mp}\;\; \text{and}\;\; r \equiv 3 \bmod 4 \\ 0\,; & \text{otherwise}\,. \end{cases} \tag{4.12}$$

The fused adjacency matrices for E_6 are given explicitly in Section 4.4.6. We shall not give the E_7 and E_8 fused adjacency explicitly, since they can be obtained straightforwardly using a computer from the recursive definition (3.18), but we note that for E_7 each entry is in $\{0,\ldots,4\}$ and that for E_8 each entry is in $\{0,\ldots,6\}$.

We now list some properties which apply to all of the A, D and E fused adjacency matrices. These properties can be proved by decomposing these matrices in terms of their eigenvalues and eigenvectors as given in [7].

For $r = g$ we have

$$F^g \;=\; 0\,. \tag{4.13}$$

Meanwhile, for $r \in \{1,\ldots,g{-}1\}$, F^r form the basis of a commutative matrix algebra, which is a representation of the Verlinde fusion algebra. These $g{-}1$ matrices are therefore often referred to as Verlinde matrices and denoted V_r.

These matrices can also be used to define related intertwiner matrices I^a, for each $a \in \mathcal{G}$, with rows labelled by $1,\ldots,g{-}1$, columns labelled by the nodes of $\mathcal{G}$ and entries given by

$$I^a_{rb} = F^r_{ab}\,. \tag{4.14}$$

Each I^a then intertwines the fused adjacency matrices of $\mathcal{G}$ and those of A_{g-1},

$$I^a\, F(\mathcal{G})^r \;=\; F(A_{g-1})^r\, I^a\,. \tag{4.15}$$

For $\mathcal{G}=A_{g-1}$, this property simply amounts to the commutation of the A_{g-1} fused adjacency matrices, but if $\mathcal{G}$ is a D or E graph it forms the basis of various relationships between $\mathcal{G}$ and the A graph with the same Coxeter number.

Finally, a property of the A, D and E fused adjacency matrices of particular relevance here is that, for $r\in\{1,\ldots,g-1\}$,

$$F^{g-r}_{ab} \;=\; F^r_{\bar{a}b} \;=\; F^r_{a\bar{b}}\,. \tag{4.16}$$

An important special case of this is $r=1$, for which

$$F^{g-1}_{ab} \;=\; \delta_{a\bar{a}}\,. \tag{4.17}$$

4.2 Bulk Weights, Fusion Matrices and Fusion Vectors

We now consider the bulk weights, fusion matrices and fusion vectors of the A, D and E models.

We see from (3.6) and (4.7) that the A_{g-1} bulk weights are

$$\begin{aligned}
W\!\left(\begin{matrix} a\pm1 & a \\ a & a\mp1\end{matrix}\,\middle|\, u\right) &= s_1(-u)\\
W\!\left(\begin{matrix} a & a\pm1 \\ a\mp1 & a\end{matrix}\,\middle|\, u\right) &= \frac{(S_{a-1}\,S_{a+1})^{1/2}\,s_0(u)}{S_a}\\
W\!\left(\begin{matrix} a & a\pm1 \\ a\pm1 & a\end{matrix}\,\middle|\, u\right) &= \frac{s_a(\pm u)}{S_a}\,.
\end{aligned} \tag{4.18}$$

It can also be shown, using (2.15), (3.8) and (4.18) together with certain results on the fusion of A_{g-1} bulk weights from [41], that the A_{g-1} fusion matrices are given explicitly by

$$P^r(a,b)_{(a,c_1,\ldots,c_{r-2},b),(a,d_1,\ldots,d_{r-2},b)} \;=$$

$$\Bigg(\prod_{m=2}^{\frac{r+a-b-1}{2}} S_m\Bigg)\Bigg(\prod_{m=2}^{\frac{r-a+b-1}{2}} S_m\Bigg)\Bigg(\prod_{m=\frac{a+b-r+1}{2}}^{\frac{a+b+r-1}{2}} S_m\Bigg)\Bigg(\prod_{m=0}^{r-1}\frac{\epsilon_{c_m}\,\epsilon_{d_m}}{(S_{c_m}\,S_{d_m})^{1/2}}\Bigg)\Bigg/\Bigg(\prod_{m=2}^{r-1} S_m\Bigg), \tag{4.19}$$

where in the fourth product we set $c_0 = d_0 = a$ and $c_{r-1} = d_{r-1} = b$, and where

$$\epsilon_a \;=\; \begin{cases} \;\;1, & a \equiv 0 \text{ or } 1 \bmod 4 \\ -1, & a \equiv 2 \text{ or } 3 \bmod 4\,. \end{cases} \tag{4.20}$$

In fact, the only properties of the sign factors required here are $\epsilon_a \in \{-1, 1\}$ and $\epsilon_{a-1}\,\epsilon_{a+1} = -1$, so any of the three other assignments which satisfy these could be used instead.

We can see from (4.19) that, in keeping with (3.20) and (4.11), each nonzero A_{g-1} fusion matrix has rank 1 and that the corresponding fusion vectors, which are thus uniquely defined up to sign, are given, up to this sign, by

$$U^r(a,b)_{1,(a,c_1,\ldots,c_{r-2},b)} \;=\; \left[\left(\prod_{m=2}^{\frac{r+a-b-1}{2}} S_m\right)\left(\prod_{m=2}^{\frac{r-a+b-1}{2}} S_m\right)\left(\prod_{m=\frac{a+b-r+1}{2}}^{\frac{a+b+r-1}{2}} S_m\right)\Big/\left(\prod_{m=2}^{r-1} S_m\right)\right]^{1/2}\left(\prod_{m=0}^{r-1}\frac{\epsilon_{c_m}}{S_{c_m}^{1/2}}\right), \tag{4.21}$$

where in the fifth product we set $c_0 = a$ and $c_{r-1} = b$.

Proceeding to $D_{\frac{g}{2}+1}$, it is possible to write expressions, similarly explicit to those for A_{g-1}, for the bulk weights and entries of the fusion matrices and fusion vectors, for a certain natural choice of these vectors. Since each of these expressions involves many different cases, analogous to those of (4.12), we do give them here. However, we note that, as with A_{g-1}, each $D_{\frac{g}{2}+1}$ bulk weight and fusion vector entry can be expressed as a single product of terms.

We also note that each $D_{\frac{g}{2}+1}$ bulk weight and fusion matrix entry can be expressed as a linear combination of A_{g-1} bulk weights and fusion matrix entries, with the coefficients being products of entries of so-called intertwiner cells. These intertwiner cells, whose exact properties are outlined in [21, 47, 48, 49], serve a similar role at the level of the bulk weights to that served at the level of the adjacency matrices by the intertwiner matrices (4.14). While the expressions provided by these intertwiner cells may not be particularly compact when applied to specific cases, they are still useful for deriving certain general properties using known properties of the intertwiner cells and of the A_{g-1} bulk weights and fusion matrices.

With regard to the E graphs, the number of different cases is particularly large so that the numerical values of fusion matrix and fusion vector entries are probably best evaluated using a computer. While this may result in a somewhat unnatural choice of the fusion vectors, this is largely immaterial since the lattice properties of interest are independent of this choice. We also note that, exactly as with $D_{\frac{g}{2}+1}$, each E bulk weight and fusion matrix entry can be expressed as a linear combination of A_{g-1} bulk weights or fusion matrix entries using intertwiner cells and that these expressions can be used to obtain general properties of the E bulk weights, fusion matrices and fusion vectors.

We now consider some properties which apply to all of the A, D and E graphs. We first note, using (4.9), that the bulk weights are invariant under the involution (4.8),

$$W\left(\begin{matrix} d & c \\ a & b \end{matrix}\,\middle|\, u\right) \;=\; W\left(\begin{matrix} \bar{d} & \bar{c} \\ \bar{a} & \bar{b} \end{matrix}\,\middle|\, u\right)\,. \tag{4.22}$$

We also see similarly that for the fusion matrices,

$$P^r(a,b)_{(a,c_1,\ldots,c_{r-2},b),(a,d_1,\ldots,d_{r-2},b)} \;=\; P^r(\bar{a},\bar{b})_{(\bar{a},\bar{c}_1,\ldots,\bar{c}_{r-2},\bar{b}),(\bar{a},\bar{d}_1,\ldots,\bar{d}_{r-2},\bar{b})}\,. \tag{4.23}$$

It follows from this that $U^r(a,b)_{\alpha,(a,c_1,\ldots,c_{r-2},b)}$ and $U^r(\bar{a},\bar{b})_{\alpha,(\bar{a},\bar{c}_1,\ldots,\bar{c}_{r-2},\bar{b})}$ correspond to two orthonormal decompositions of both $P^r(a,b)$ and $P^r(\bar{a},\bar{b})$, and therefore that these fusion vectors are related by a transformation (3.26),

$$U^r(\bar{a},\bar{b})_{\alpha,(\bar{a},\bar{c}_1,\ldots,\bar{c}_{r-2},\bar{b})} \;=\; \sum_{\alpha'=1}^{F^r_{ab}} R^r(a,b)_{\alpha\alpha'}\; U^r(a,b)_{\alpha',(a,c_1,\ldots,c_{r-2},b)}\,. \tag{4.24}$$

Finally, we note that the fusion matrices $P^{g-1}(a,\bar{a})$, which from (4.17) all have rank 1, can be used to generate the fusion matrices of lower fusion level according to

$$\begin{aligned}\sum_{(b,e_1,\ldots,e_{g-r-2},\bar{a})\,\in\,\mathcal{G}^{g-r}_{b\bar{a}}} & P^{g-1}(a,\bar{a})_{(a,c_1,\ldots,c_{r-2},b,e_1,\ldots,e_{g-r-2},\bar{a}),(a,d_1,\ldots,d_{r-2},b,e_1,\ldots,e_{g-r-2},\bar{a})} \\ & = \frac{\psi_b}{S_r\,\psi_a}\, P^r(a,b)_{(a,c_1,\ldots,c_{r-2},b),(a,d_1,\ldots,d_{r-2},b)}\,.\end{aligned} \tag{4.25}$$

This can be proved by first obtaining the result for the A graphs using (4.19) and then proceeding to the D and E graphs using intertwiner cells.

4.3 Additional Boundary Condition and Transfer Matrix Properties

We now show that in addition to satisfying all of the properties outlined in Section 3.8, including those of Section 3.8.10 arising from bicolourability with parity (4.10), the A–D–E models possess further important symmetries associated with the involutions (4.8) and the intertwiner relations (4.14).

4.3.1 Symmetry under $a_1 \mapsto \bar{a}_1$ and $a_2 \mapsto \bar{a}_2$

We first consider the relationship between the (r,a) and $(r,\bar{a})$ boundary conditions. It follows straightforwardly from (4.16) and (3.42) that the sets of boundary edges for these boundary conditions are related by

$$\mathcal{E}^{r\bar{a}} \;=\; \{(\bar{b},\bar{c})\,|\,(b,c)\in\mathcal{E}^{ra}\}\,. \tag{4.26}$$

Proceeding to the corresponding boundary edge weights and boundary weights, we find, using (4.24), that

$$E^{r\bar{a}}(\bar{b},\bar{c})_{\beta\gamma} \;=\; \sum_{\beta'=1}^{F^r_{ba}}\sum_{\gamma'=1}^{F^{r+1}_{ca}} S^{ra}(b)_{\beta\beta'}\; S^{r+1,a}(c)_{\gamma\gamma'}\; E^{ra}(b,c)_{\beta'\gamma'} \tag{4.27}$$

and

$$B^{r\bar{a}}\!\left(\bar{c}\;\begin{matrix}\bar{d}&\delta\\ \bar{b}&\beta\end{matrix}\,\middle|\,u,\xi\right) \;=\; \sum_{\beta'=1}^{F^r_{ba}}\sum_{\delta'=1}^{F^r_{da}} S^{ra}(b)_{\beta\beta'}\; S^{ra}(d)_{\delta\delta'}\; B^{ra}\!\left(c\;\begin{matrix}d&\delta'\\ b&\beta'\end{matrix}\,\middle|\,u,\xi\right), \tag{4.28}$$

where the orthonormal transformation matrices in (4.24) and those in (4.27) and (4.28) are related by (3.38).

It now follows from (4.22) and (4.28) that $\boldsymbol{D}^N_{r_1\bar{a}_1|r_2\bar{a}_2}(u,\xi_1,\xi_2)$ and $\boldsymbol{D}^N_{r_1a_1|r_2a_2}(u,\xi_1,\xi_2)$ are related by a similarity transformation,

$$\begin{aligned}\boldsymbol{D}^N_{r_1\bar{a}_1|r_2\bar{a}_2}(u,\xi_1,\xi_2)\;\boldsymbol{H}^N_{r_1a_1|r_2a_2}\;\boldsymbol{S}^N_{r_1a_1|r_2a_2} \;&=\\ &\boldsymbol{H}^N_{r_1a_1|r_2a_2}\;\boldsymbol{S}^N_{r_1a_1|r_2a_2}\;\boldsymbol{D}^N_{r_1a_1|r_2a_2}(u,\xi_1,\xi_2)\,,\end{aligned} \tag{4.29}$$

where $\boldsymbol{S}^N_{r_1a_1|r_2a_2}$ is given by (3.63), using the same $S^{ra}(e)$ as in (4.28), and $\boldsymbol{H}^N_{r_1a_1|r_2a_2}$ is a square matrix with rows labelled by the paths of $\mathcal{G}^N_{r_1\bar{a}_1|r_2\bar{a}_2}$, columns labelled by the paths of $\mathcal{G}^N_{r_1a_1|r_2a_2}$ and entries given by

$$\boldsymbol{H}^N_{r_1a_1|r_2a_2\;(\beta_1,b_0,\ldots,b_N,\beta_2),(\delta_1,d_0,\ldots,d_N,\delta_2)} \;=\; \delta_{(\beta_1,\bar{b}_0,\ldots,\bar{b}_N,\beta_1),(\delta_1,d_0,\ldots,d_N,\delta_2)}\,. \tag{4.30}$$

4.3.2 Equivalence of (r,a) and $(g-r-1,\bar{a})$ Boundary Conditions at the Conformal Point

We now show that, at the conformal point and for $r\in\{1,\ldots,g-2\}$, the (r,a) and $(g-r-1,\bar{a})$ boundary conditions are equivalent. This equivalence takes the form of the boundary edge weights for each of these boundary conditions being the same, except for a gauge transformation and a reversal of the order of the nodes in each boundary pair, neither of which affects any properties of interest. We shall denote such an equivalence of boundary conditions by $\leftrightarrow$.

In terms of the set of boundary edges (3.42), it follows from (4.16) that, for $r\in\{1,\ldots,g-2\}$, the sets $\mathcal{E}^{ra}$ and $\mathcal{E}^{g-r-1,\bar{a}}$ contain the same pairs of nodes but with opposite ordering; that is,

$$\mathcal{E}^{g-r-1,\bar{a}} \;=\; \{(c,b)\,|\,(b,c)\in\mathcal{E}^{ra}\}\,. \tag{4.31}$$

We also see, from (4.13), that

$$\mathcal{E}^{g-1,a} \;=\; \emptyset\,, \tag{4.32}$$

so that at the conformal point there are no $(g-1,a)$ boundary conditions.

For the boundary edge weights, the equivalence of the (r,a) and $(g-r-1,\bar{a})$ boundary conditions is

$$E^{g-r-1,\bar{a}}(c,b)_{\gamma\beta} \;=\; \sum_{\beta'=1}^{F^r_{ba}}\;\sum_{\gamma'=1}^{F^{r+1}_{ca}}\; S^{ra}(b)_{\beta\beta'}\;S^{r+1,a}(c)_{\gamma\gamma'}\;E^{ra}(b,c)_{\beta'\gamma'}\,, \tag{4.33}$$

where $S^{ra}(e)$ are orthonormal matrices satisfying (3.37) which are defined by

$$\begin{aligned} S^{ra}(e)_{\alpha\alpha'} \;=\; &(S_r\,\psi_a\,/\psi_e)^{1/2}\times\\ &\sum_{(e,b_1,\ldots,b_{g-r-2},\bar{a})\,\in\,\mathcal{G}^{g-r}_{e\bar{a}}}\;\sum_{(e,c_1,\ldots,c_{r-2},a)\,\in\,\mathcal{G}^r_{ea}} U^{g-1}(\bar{a},a)_{1,(\bar{a},b_{g-r-2},\ldots,b_1,e,c_1,\ldots,c_{r-2},a)}\times\\ &\qquad U^{g-r}(e,\bar{a})_{\alpha,(e,b_1,\ldots,b_{g-r-2},\bar{a})}\;U^r(e,a)_{\alpha',(e,c_1,\ldots,c_{r-2},a)}\,. \end{aligned} \tag{4.34}$$

We note that $S^{ra}(e)$ also satisfy

$$S^{ra}(e)^T \;=\; S^{g-r,\bar{a}}(e)\,. \tag{4.35}$$

These relations, (4.33) and (4.35), and the orthonormality (3.37) can all be proved using the general properties of the fusion matrices and fusion vectors, (3.15), (3.16), (3.22), (3.23) and those which follow from (2.17), together with (4.25).

We now note that, as labels, (r,a) and $(g-r-1,\bar{a})$ are always distinct since for an $A_{\rm odd}$, D or E graph g is even so that r and $g-r-1$ are different, while for an $A_{\rm even}$ graph g is odd so that a and $\bar{a}=g-a$ are different. Thus, due to the equivalence (4.33), there are at most $(g-2)\,|\mathcal{G}|/2$ distinct boundary conditions. Furthermore, by examining the sets of boundary edges (3.42) for each A, D and E case, we find that there are no further equivalences between these sets, either direct or through reversing the order of nodes in each edge. We therefore conclude that

$$\text{number of boundary conditions at the conformal point} \;=\; (g-2)\,|\mathcal{G}|/2\,. \tag{4.36}$$

Due to the consistency condition (3.79), the implementation of a given left and right boundary condition at their conformal points on a lattice of fixed width can be achieved using only two of the four possibilities which arise from the two versions of each boundary condition. If (r_1,a_1) and (r_2,a_2) is one of these possibilities, then the other is $(g-r_1-1,\bar{a}_1)$ and $(g-r_2-1,\bar{a}_2)$ and the transfer matrices for the two are related by

$$\begin{aligned}&\boldsymbol{D}^N_{g-r_1-1,\bar{a}_1|g-r_2-1,\bar{a}_2}(\xi,\lambda-\xi,\xi) \;=\\ &\qquad \boldsymbol{S}^N_{r_1+1,a_1|r_2+1,a_2}\;\hat{\boldsymbol{T}}^N_{r_1a_1|r_2a_2}(\lambda-\xi)\;\check{\boldsymbol{T}}^N_{r_1a_1|r_2a_2}(\lambda-\xi)\;(\boldsymbol{S}^N_{r_1+1,a_1|r_2+1,a_2})^{-1}\,,\end{aligned} \tag{4.37}$$

where $\boldsymbol{S}^N_{r_1+1,a_1|r_2+1,a_2}$ is given by (3.63) and (4.33). Comparing this with (3.75) we see that the ordering in the products of single row transfer matrices is different in each, which does not affect the nonzero eigenvalues (although unimportant differences in the number of zero eigenvalues will arise due to the different dimensions of the oppositely-ordered products). We thus see that the partition functions are related by

$$\boldsymbol{Z}^{NM}_{g-r_1-1,\bar{a}_1|g-r_2-1,\bar{a}_2}(\xi,\lambda-\xi,\xi) \;=\; \boldsymbol{Z}^{NM}_{r_1a_1|r_2a_2}(\lambda-\xi,\xi,\lambda-\xi)\,. \tag{4.38}$$

Finally, we find, using (2.30) in(3.29), that the boundary edge weight relation (4.33) implies the boundary weight relation

$$B^{g-r,\bar{a}}\left(c\ \begin{matrix} d & \delta \\ b & \beta \end{matrix}\ \middle|\ u,\xi\right) \;=\; \sum_{\beta'=1}^{F^r_{ba}} \sum_{\delta'=1}^{F^r_{da}} S^{ra}(b)_{\beta\beta'}\, S^{ra}(d)_{\delta\delta'}\, B^{ra}\left(c\ \begin{matrix} d & \delta' \\ b & \beta' \end{matrix}\ \middle|\ u,-\xi\right), \qquad (4.39)$$

with $S^{ra}(e)$ again given by (4.34). This then implies that

$$\boldsymbol{Z}^{NM}_{r_1a_1|r_2a_2}(u,\xi_1,\xi_2) \;=\; \boldsymbol{Z}^{NM}_{g-r_1,\bar{a}_1|r_2a_2}(u,-\xi_1,\xi_2) \;=\; \boldsymbol{Z}^{NM}_{r_1a_1|g-r_2,\bar{a}_2}(u,\xi_1,-\xi_2)\,. \qquad (4.40)$$

This relation taken at $u=\lambda-\xi_1=\xi_2=\lambda-\xi$ is consistent with (4.38) through the equivalence, which follows from (3.49), of the (r,a) boundary condition at $u=-\xi$ and the $(r-1,a)$ boundary condition at $u=\xi$.

4.3.3 Intertwiner Symmetry

We now consider the relationship between the double-row transfer matrices and partition functions of the model based on $\mathcal{G}$, with Coxeter number g, and those of the model based on A_{g-1}. In particular, we shall find that any A–D–E partition function can be expressed as a sum of certain A partition functions.

It can be shown using intertwiner cells that, for each $r_1, r_2, s' \in \{1,\ldots,g-1\}$ and $a_1, a_2 \in \mathcal{G}$, we have

$$\begin{aligned} \bigoplus_{a\in\mathcal{G}}^{F^{s'}_{a_1a}} \boldsymbol{D}^{N}_{r_1a|r_2a_2}(u,\xi_1,\xi_2) \;&\approx\; \bigoplus_{s=1}^{g-1}{}^{F^{s}_{a_1a_2}} \boldsymbol{D}^{N,\,A_{g-1}}_{r_1s'|r_2s}(u,\xi_1,\xi_2) \\ \bigoplus_{a\in\mathcal{G}}^{F^{s'}_{a_2a}} \boldsymbol{D}^{N}_{r_1a_1|r_2a}(u,\xi_1,\xi_2) \;&\approx\; \bigoplus_{s=1}^{g-1}{}^{F^{s}_{a_1a_2}} \boldsymbol{D}^{N,\,A_{g-1}}_{r_1s|r_2s'}(u,\xi_1,\xi_2)\,, \end{aligned} \qquad (4.41)$$

where we are using $\approx$ and the superscripts on $\oplus$ in the same ways as in (3.71), and where the fused adjacency matrices on both sides and the transfer matrices on the left sides refer to $\mathcal{G}$, while the transfer matrices on the right sides refer, as indicated, to A_{g-1}.

Since the two forms of this relation can be proved similarly, and are related through the symmetries of Sections 3.8.6 and 3.8.7, we shall consider, from now on, only the first form.

We now discuss the details of the proof. The similarity transformation in the first line of (4.41) can be implemented by an invertible matrix $\boldsymbol{J}^{s'N}_{r_1a_1|r_2a_2}$ which premultiplies the left side and postmultiplies the right side. The rows of $\boldsymbol{J}^{s'N}_{r_1a_1|r_2a_2}$ and the rows and columns of $\bigoplus_{s=1}^{g-1} F^s_{a_1a_2}\boldsymbol{D}^{N,\,A_{g-1}}_{r_1s'|r_2s}(u,\xi_1,\xi_2)$ are labelled by the paths of

$$\Big\{(t_0,\ldots,t_N,t,\alpha_2)\,\Big|\,(1,t_0,\ldots,t_N,1)\in(A_{g-1})^N_{r_1s'|r_2t},\; F^t_{a_1a_2}>0,\; \alpha_2\in\{1,\ldots,F^t_{a_1a_2}\}\Big\}\,,$$

while the columns of $\boldsymbol{J}^{s'N}_{r_1a_1|r_2a_2}$ and the rows and columns of $\bigoplus_{a\in\mathcal{G}} F^{s'}_{a_1a}\boldsymbol{D}^N_{r_1a|r_2a_2}(u,\xi_1,\xi_2)$ are labelled by the paths of

$$\Big\{(\alpha_1,b,\beta_1,b_0,\ldots,b_N,\beta_2)\,\Big|\,(\beta_1,b_0,\ldots,b_N,\beta_2)\in\mathcal{G}^N_{r_1b|r_2a_2},\; F^{s'}_{a_1b}>0,\; \alpha_1\in\{1,\ldots,F^{s'}_{a_1b}\}\Big\}\,.$$

The entries of these matrices are given by

$$\begin{aligned}
&\boldsymbol{J}^{s'N}_{r_1a_1|r_2a_2\;(t_0,\ldots,t_N,t,\alpha_2),(\alpha_1,b,\beta_1,b_0,\ldots,b_N,\beta_2)} \;=\\
&\qquad\sum_{\gamma_0=1}^{F^{t_0}_{a_1b_0}}\cdots\sum_{\gamma_N=1}^{F^{t_N}_{a_1b_N}} Q^{r_1a_1}\!\begin{pmatrix} b & \beta_1 & b_0\\ \alpha_1 & & \gamma_0\\ s' & 1 & t_0\end{pmatrix}\left[\prod_{j=0}^{N-1} Q^{a_1}\!\begin{pmatrix} b_j & b_{j+1}\\ \gamma_j & \gamma_{j+1}\\ t_j & t_{j+1}\end{pmatrix}\right] Q^{r_2a_1}\!\begin{pmatrix} b_N & \beta_2 & a_2\\ \gamma_N & & \alpha_2\\ t_N & 1 & t\end{pmatrix}\,,
\end{aligned}\tag{4.42}$$

$$\begin{aligned}
&\left[\bigoplus_{a\in\mathcal{G}} F^{s'}_{a_1a}\;\boldsymbol{D}^N_{r_1a|r_2a_2}(u,\xi_1,\xi_2)\right]_{(\alpha_1,b,\beta_1,b_0,\ldots,b_N,\beta_2),(\alpha_1',d,\delta_1,d_0,\ldots,d_N,\delta_2)} \;=\\
&\qquad\qquad \delta_{\alpha_1\alpha_1'}\;\delta_{bd}\;\boldsymbol{D}^N_{r_1b|r_2a_2}(u,\xi_1,\xi_2)_{(\beta_1,b_0,\ldots,b_N,\beta_2),(\delta_1,d_0,\ldots,d_N,\delta_2)}
\end{aligned}\tag{4.43}$$

and similarly for $\bigoplus_{s=1}^{g-1} F^s_{a_1a_2}\boldsymbol{D}^{N,\,A_{g-1}}_{r_1s'|r_2s}(u,\xi_1,\xi_2)$. In (4.42), Q^{a_1} are intertwiner cells associated with the intertwiner matrix I^{a_1} of (4.14), and $Q^{r_1a_1}$ and $Q^{r_2a_1}$ are fused blocks of such cells, of widths r_1-1 and r_2-1 respectively. Thus, $\boldsymbol{J}^{s'N}_{r_1a_1|r_2a_2}$ can be viewed as a row of intertwiner cells in which the spins on the lower left and upper right corners are fixed to s' and a_2 respectively, the lower row of spins between s' and a_2 on A_{g-1} label the rows of the matrix and the upper row of spins between s' and a_2 on $\mathcal{G}$ label the columns of the matrix. We also see that all of the matrices here are square with dimension $(I^{a_1}F^{r_1}G^NF^{r_2})_{s'a_2}$, it being possible using (4.15) to propagate I^{a_1} to the right of this expression while replacing the adjacency matrices of $\mathcal{G}$ with those of A_{g-1}. The intertwiner cells are assumed to satisfy an intertwiner relation, as given in (4.6a) of [47], as well as two inversion relations, as given in (4.6b) and (4.6c) of [47]. It follows immediately from the inversion relations that $\boldsymbol{J}^{s'N}_{r_1a_1|r_2a_2}$ is invertible, with its inverse being given, up to gauge transformations on the intertwiner cells, by its transpose. Meanwhile, the equation corresponding to the first line of (4.41) can be obtained by using one of the inversion relations to insert a pair of cells between $\boldsymbol{J}^{s'N}_{r_1a_1|r_2a_2}$ and $\bigoplus_{a\in\mathcal{G}} {}^{F^{s'}_{a_1a}}\boldsymbol{D}^N_{r_1a|r_2a_2}(u,\xi_1,\xi_2)$, using the intertwiner relation and the form (3.33) of the boundary weights to propagate these cells around a single loop, and then using an inversion relation again to remove the inserted cells, thus giving $\bigoplus_{s=1}^{g-1} {}^{F^s_{a_1a_2}}\boldsymbol{D}^{N,\,A_{g-1}}_{r_1s'|r_2s}(u,\xi_1,\xi_2)\,\boldsymbol{J}^{s'N}_{r_1a_1|r_2a_2}$ and completing the proof. We observe that this last process is similar to that which occurs in the proof, mentioned in Section 3.8.1, of the commutation of double-row transfer matrices, the commutation proof involving the insertion of two pairs of bulk weights which are propagated around two loops.

We note that (4.41) is still nontrivial for $\mathcal{G}=A_{g-1}$ and that it then corresponds to certain cases of (3.71). In fact, the A_{g-1} intertwiner cells Q^a can be obtained by taking a $u\to i\infty$ limit on fused $a-1$ by 1 blocks of A_{g-1} bulk weights.

We also note that the intertwiner cells Q^a for $\mathcal{G}$ a D or E graph have only been found explicitly, in [21, 47, 48, 49], for $a=1$. However, for various reasons, the existence of these cells for other values of a seems guaranteed.

Finally, we observe that a particularly important case of (4.41) is $s'=1$, for which

$$\boldsymbol{D}^N_{r_1a_1|r_2a_2}(u,\xi_1,\xi_2) \;\approx\; \bigoplus_{s=1}^{g-1} {}^{F^s_{a_1a_2}}\;\boldsymbol{D}^{N,\,A_{g-1}}_{r_11|r_2s}(u,\xi_1,\xi_2)\,, \tag{4.44}$$

which in turn implies that

$$\boldsymbol{Z}^{NM}_{r_1a_1|r_2a_2}(u,\xi_1,\xi_2) \;=\; \sum_{s=1}^{g-1} F^s_{a_1a_2}\;\boldsymbol{Z}^{NM,\,A_{g-1}}_{r_11|r_2s}(u,\xi_1,\xi_2)\,. \tag{4.45}$$

We thus see that the task of evaluating the partition functions of all of the A–D–E models with boundary conditions (r_1,a_1) and (r_2,a_2) has been reduced to that of evaluating the partition functions of just the A models with boundary conditions $(r_1,1)$ and (r_2,s).

4.4 Boundary Weights

We now consider the explicit forms of the boundary weights and boundary edge weights for the A–D–E models.

4.4.1 A Graphs

For A_{g-1}, we find, using (4.21) in (3.43) and then applying a simple gauge transformation to remove a factor ϵ_c which arises, that the boundary edge weights are given explicitly by

$$E^{ra}(c\pm1,c)_{11} \;=\; \frac{(S_{(r\mp c+a)/2}\,S_{(c\pm a\mp r)/2})^{1/2}}{(S_{c\pm1}\,S_c)^{1/4}}\,. \tag{4.46}$$

We see that each of these weights is positive. We also see that, for these weights, the relations (4.27) and (4.33) are

$$E^{r,g-a}(g-b,g-c)_{11} \;=\; E^{ra}(b,c)_{11}\,, \quad E^{g-r-1,g-a}(c,b)_{11} \;=\; E^{ra}(b,c)_{11}\,. \tag{4.47}$$

Substituting (4.46) into (3.47) we now find that the A_{g-1} boundary weights are

$$B^{ra}\!\left(c\;\begin{matrix}c\pm1 & 1\\ c\pm1 & 1\end{matrix}\;\middle|\;u,\xi\right) \;=$$

$$\frac{S_{(r\mp c+a)/2}\,S_{(c\pm a\mp r)/2}\,s_0(\xi+u)\,s_r(\xi-u)+S_{(r\pm c+a)/2}\,S_{(c\mp a\pm r)/2}\,s_0(\xi-u)\,s_r(\xi+u)}{S_r\,(S_c\,S_{c\pm1})^{1/2}\,s_0(2\xi)} \tag{4.48}$$

$$B^{ra}\!\left(c\;\begin{matrix}c\mp1 & 1\\ c\pm1 & 1\end{matrix}\;\middle|\;u,\xi\right) \;=\; \frac{(S_{(r-c+a)/2}\,S_{(r+c-a)/2}\,S_{(c+a-r)/2}\,S_{(c+a+r)/2})^{1/2}\,s_0(2u)}{(S_{c-1}\,S_{c+1})^{1/4}\,S_c^{1/2}\,s_0(2\xi)}\,.$$

All of the boundary weights which were found as solutions of the boundary Yang-Baxter equation for the A_{g-1} models and their off-critical extensions in [4, 29, 30, 31, 32, 33] can be related to those of (4.48) by using appropriate values for the various parameters involved. In particular, we note that more general boundary weights which depend on two boundary field parameters are known, as for example given in (3.14–3.15) of [4], and that these reduce to the weights (4.48) when one of these parameters is set to $i\infty$.

Some important special cases here are the $(r,1)$ and $(g-r-1,g-1)$ boundary conditions for which

$$\begin{aligned} \mathcal{E}^{r1} \;&=\; \{(r,r{+}1)\}\,, \qquad \mathcal{E}^{g-r-1,g-1} \;=\; \{(r{+}1,r)\}\,, \\ E^{r1}(r,r{+}1) \;&=\; E^{g-r-1,g-1}(r{+}1,r) \;=\; (S_r\,S_{r+1})^{1/4}\,. \end{aligned} \tag{4.49}$$

The corresponding boundary weights are all diagonal and given by

$$\begin{aligned} B^{r1}\!\left(r{\pm}1\;\begin{matrix} r & 1 \\ r & 1 \end{matrix}\;\middle|\; u,\xi\right) \;=\; B^{g-r,g-1}\!\left(r{\pm}1\;\begin{matrix} r & 1 \\ r & 1 \end{matrix}\;\middle|\; u,-\xi\right) \;=& \\ \frac{S_{r\pm1}^{1/2}\;s_0(\xi{\pm}u)\;s_r(\xi{\mp}u)}{S_r^{1/2}\;s_0(2\xi)}\,,& \end{aligned} \tag{4.50}$$

these weights matching those found in [31]. We see that for $r\in\{2,\ldots,g-2\}$ these cases provide an example in which boundary weights which are nonzero away from the conformal point vanish at the conformal point. More specifically, away from the conformal point, these cases represent semi-fixed boundary conditions in which the state of every alternate boundary spin is fixed to be r and that of each spin between these can be $r-1$ or $r+1$, while at the conformal point they represent completely fixed boundary conditions in which only a single boundary spin configuration $\ldots r,r+1,r,r+1\ldots$ contributes to the partition function.

Other important cases here are the $(1,a)\leftrightarrow(g-2,g-a)$ boundary conditions, with $a\in\{2,\ldots,g-2\}$, for which

$$\begin{aligned} \mathcal{E}^{1a} \;&=\; \{(a,a{-}1),(a,a{+}1)\}\,, \quad \mathcal{E}^{g-2,g-a} \;=\; \{(a{-}1,a),(a{+}1,a)\}\,, \\ E^{1a}(a,a{\pm}1) \;&=\; E^{g-2,g-a}(a{\pm}1,a) \;=\; (S_{a\pm1}/S_a)^{1/4}\,. \end{aligned} \tag{4.51}$$

As already seen for the general case in (3.32), these are semi-fixed boundary conditions in which the state of every alternate boundary spin is fixed to be a.

We now observe that the only cases in which every edge of A_{g-1} appears, in one order, in the set of boundary edges are

$$\begin{aligned} g \text{ odd:} \quad & \begin{cases} \mathcal{E}^{\frac{g-1}{2},\frac{g-1}{2}} = \{(1,2),(3,2),\ldots,(g-2,g-3),(g-2,g-1)\} \\ \mathcal{E}^{\frac{g-1}{2},\frac{g+1}{2}} = \{(2,1),(2,3),\ldots,(g-3,g-2),(g-1,g-2)\} \end{cases} \\ g \text{ even:} \quad & \begin{cases} \mathcal{E}^{\frac{g}{2}-1,\frac{g}{2}} = \{(2,1),(2,3),\ldots,(g-2,g-3),(g-2,g-1)\} \\ \mathcal{E}^{\frac{g}{2},\frac{g}{2}} = \{(1,2),(3,2),\ldots,(g-3,g-2),(g-1,g-2)\}\,. \end{cases} \end{aligned} \tag{4.52}$$

These cases therefore represent boundary conditions in which each configuration of boundary spins consistent with fixed even-spin and odd-spin sublattices contributes a nonzero weight to the partition function at the conformal point. If these weights are all equal, which in fact only occurs for A_3, we refer to the boundary condition as free, while if the weights are not all equal we refer to it as quasi-free.

Finally, we note that all other boundary conditions not of the fixed, semi-fixed, quasi-free or free type can be regarded as intermediate between these types.

4.4.2 Example: A_3

We now consider, as an example, the case A_3. For any spin assignment in the A_3 model, the spin states on one sublattice are all 2, while each spin state on the other is either 1 or 3. The former sublattice, being frozen in a single configuration, can therefore be discarded and the model viewed as a two-state model on the other sublattice. It can be shown that the bulk weights of this model are those of the critical Ising model, with the horizontal and vertical coupling constants suitably parameterised in terms of the spectral parameter. It is therefore natural to relabel the nodes of A_3 as a frozen state 0 and Ising states $+$ and $-$; that is,

$A_3 \quad = $ 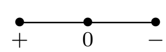 . (4.53)

The A_3 fused adjacency matrices are, from (4.11),

$$F^1 = \begin{pmatrix} 1&0&0\\0&1&0\\0&0&1 \end{pmatrix} \quad F^2 = \begin{pmatrix} 0&1&0\\1&0&1\\0&1&0 \end{pmatrix} \quad F^3 = \begin{pmatrix} 0&0&1\\0&1&0\\1&0&0 \end{pmatrix} \quad F^4 = \begin{pmatrix} 0&0&0\\0&0&0\\0&0&0 \end{pmatrix}. \tag{4.54}$$

Using these matrices to determine each set of boundary edges and then (4.46) to give the corresponding weights, we find that these weights are, up to normalisation, as given in Table 1.

$-$	$E(-,0)_{11} = 1$	$E(0,+)_{11} = 1$
0	$E(0,+)_{11} = E(0,-)_{11} = 1$	$E(+,0)_{11} = E(-,0)_{11} = 1$
$+$	$E(+,0)_{11} = 1$	$E(0,-)_{11} = 1$
a / r	1	2

Table 1: A_3 boundary edge weights

We see that the three A_3 boundary conditions at the conformal point are:

- $(1,+) \ \leftrightarrow \ (2,-) \ \leftrightarrow \ +$ fixed
- $(1,-) \ \leftrightarrow \ (2,+) \ \leftrightarrow \ -$ fixed
- $(1,0) \ \leftrightarrow \ (2,0) \ \leftrightarrow$ free.

We note that the last of these boundary conditions is invariant under the model's $\mathbb{Z}_2$ symmetry, while the first two are not.

4.4.3 Example: A_4

We now consider, as another example, the case A_4. It is known that this model can related to the tricritical hard square and tricritical Ising models.

The A_4 fused adjacency matrices are

$$F^1 = \begin{pmatrix} 1&0&0&0\\ 0&1&0&0\\ 0&0&1&0\\ 0&0&0&1 \end{pmatrix} \quad F^2 = \begin{pmatrix} 0&1&0&0\\ 1&0&1&0\\ 0&1&0&1\\ 0&0&1&0 \end{pmatrix} \quad F^3 = \begin{pmatrix} 0&0&1&0\\ 0&1&0&1\\ 1&0&1&0\\ 0&1&0&0 \end{pmatrix}$$
$$F^4 = \begin{pmatrix} 0&0&0&1\\ 0&0&1&0\\ 0&1&0&0\\ 1&0&0&0 \end{pmatrix} \quad F^5 = \begin{pmatrix} 0&0&0&0\\ 0&0&0&0\\ 0&0&0&0\\ 0&0&0&0 \end{pmatrix}. \tag{4.55}$$

Using these and (4.46), we find that the A_4 boundary edge weights are, up to normalisation, as given in Table 2.

$a \backslash r$	1	2	3
4	$E(4,3)_{11} = 1$	$E(3,2)_{11} = 1$	$E(2,1)_{11} = 1$
3	$E(3,2)_{11} = (\sqrt{5}+1)^{1/8}$ $E(3,4)_{11} = (\sqrt{5}-1)^{1/8}$	$E(2,1)_{11} = E(4,3)_{11}$ $= (\sqrt{5}+1)^{1/8}$ $E(2,3)_{11} = (5\sqrt{5}-11)^{1/8}$	$E(1,2)_{11} = (\sqrt{5}-1)^{1/8}$ $E(3,2)_{11} = (\sqrt{5}+1)^{1/8}$
2	$E(2,1)_{11} = (\sqrt{5}-1)^{1/8}$ $E(2,3)_{11} = (\sqrt{5}+1)^{1/8}$	$E(1,2)_{11} = E(3,4)_{11}$ $= (\sqrt{5}+1)^{1/8}$ $E(3,2)_{11} = (5\sqrt{5}-11)^{1/8}$	$E(2,3)_{11} = (\sqrt{5}+1)^{1/8}$ $E(4,3)_{11} = (\sqrt{5}-1)^{1/8}$
1	$E(1,2)_{11} = 1$	$E(2,3)_{11} = 1$	$E(3,4)_{11} = 1$

Table 2: A_4 boundary edge weights

We see that the six A_4 boundary conditions at the conformal point are:

- $(1,1) \leftrightarrow (3,4) \leftrightarrow \ldots 1,2,1,2\ldots$ fixed
- $(1,4) \leftrightarrow (3,1) \leftrightarrow \ldots 3,4,3,4\ldots$ fixed
- $(2,1) \leftrightarrow (2,4) \leftrightarrow \ldots 2,3,2,3\ldots$ fixed
- $(1,2) \leftrightarrow (3,3) \leftrightarrow \ldots 2,1/3,2,1/3\ldots$ semi-fixed
- $(1,3) \leftrightarrow (3,2) \leftrightarrow \ldots 3,2/4,3,2/4\ldots$ semi-fixed
- $(2,2) \leftrightarrow (2,3) \leftrightarrow$ quasi-free.

4.4.4 D Graphs

For $D_{\frac{g}{2}+1}$, we find, by substituting the fusion vector entries described in Section 4.2 into (3.43) and then applying certain simple gauge transformations, that the boundary edge weights can be taken explicitly as

$$E^{ra}(b,c)_{11} = \begin{cases} 2^{-1/4}|_{b,c=\frac{g}{2}} \;\; E_A^{ra}(b,c)_{11}\,; \;\; a\neq \frac{g}{2}\,,\;\; r\leq \frac{g}{2}-1 \\ 2^{-1/4}|_{b,c=\frac{g}{2}} \;\; E_A^{r,g-a}(b,c)_{11}\,; \;\; a\neq \frac{g}{2}\,,\;\; r\geq \frac{g}{2} \\ 2^{1/4}|_{b,c=\frac{g}{2}} \;\; E_A^{r,\frac{g}{2}}(b,c)_{11}\,; \;\; a= \frac{g}{2} \end{cases}$$

$$E^{ra}(b,c)_{12} = \begin{cases} 0\,; \;\; b\neq \frac{g}{2} \\ \pm 2^{-1/4} \;\; E_A^{r,g-a}(\frac{g}{2},\frac{g}{2}-1)_{11}\,; \;\; b=\frac{g}{2}^{\pm},\;\; r\leq \frac{g}{2}-1 \\ \pm 2^{-1/4} \;\; E_A^{ra}(\frac{g}{2},\frac{g}{2}-1)_{11}\,; \;\; b=\frac{g}{2}^{\pm},\;\; r\geq \frac{g}{2} \end{cases} \tag{4.56}$$

$$E^{ra}(b,c)_{21} = \begin{cases} 0\,; \;\; c\neq \frac{g}{2} \\ \pm 2^{-1/4} \;\; E_A^{r,g-a}(\frac{g}{2}-1,\frac{g}{2})_{11}\,; \;\; c=\frac{g}{2}^{\pm},\;\; r\leq \frac{g}{2}-1 \\ \pm 2^{-1/4} \;\; E_A^{ra}(\frac{g}{2}-1,\frac{g}{2})_{11}\,; \;\; c=\frac{g}{2}^{\pm},\;\; r\geq \frac{g}{2} \end{cases}$$

$$E^{ra}(b,c)_{22} = \begin{cases} E_A^{r,g-a}(b,c)_{11}\,; \;\; r\leq \frac{g}{2}-1 \\ E_A^{ra}(b,c)_{11}\,; \;\; r\geq \frac{g}{2}\,, \end{cases}$$

where by $X|_{b,c=\frac{g}{2}}$ we mean that X is only to be included if $b=\frac{g}{2}$ or $c=\frac{g}{2}$, and where $E_A^{ra}(b,c)_{11}$ are the A_{g-1} boundary edge weights as given by (4.46). The fact that the $D_{\frac{g}{2}+1}$ boundary edge weights can be expressed in terms of A_{g-1} boundary edge weights follows from the intertwiner relations between the corresponding models.

We see that for any boundary condition, and in this gauge, there is at most one negative boundary edge weight. We also see that, for these weights, the relations (4.27) and (4.33) are

$$E^{r\bar{a}}(\bar{b},\bar{c})_{\beta\gamma} \;=\; \sigma_{\beta\gamma}\, E^{ra}(b,c)_{\beta\gamma}\,, \qquad E^{g-r-1,\bar{a}}(c,b)_{\gamma\beta} \;=\; E^{ra}(b,c)_{\beta\gamma}\,, \tag{4.57}$$

where

$$\sigma_{\beta\gamma} \;=\; \begin{cases} -1, & D_{\text{odd}} \text{ with } \beta\neq\gamma \\ \;\;\,1, & \text{otherwise.} \end{cases} \tag{4.58}$$

In fact, for D_{even} the first relation of (4.57) is trivial since the involution $a\mapsto\bar{a}$ is the identity, but we note that the relation still holds if the involution is instead taken to be the graph's $\mathbb{Z}_2$ symmetry transformation and if $\sigma_{12}=\sigma_{21}$ are replaced by -1.

Boundary weights for $D_{\frac{g}{2}+1}$ can be obtained by substituting the edge weights (4.56) into (3.47). For some of the boundary conditions, all of the boundary weights are diagonal and these weights can be related to those previously found in [32]. However, non-diagonal boundary weights for the $D_{\frac{g}{2}+1}$ models, apart from one case of D_4 considered in [5], were not previously known. We also note that since some simple, but (r,a)-dependent, gauge transformations have been included in the boundary edge weights of (4.56), some corresponding gauge factors need to be included in equations which relate boundary weights at different values of (r,a), in particular (3.49) and (4.39).

Finally, we note that, as with A_{g-1}, certain of the $D_{\frac{g}{2}+1}$ boundary conditions can be identified as being of fixed, semi-fixed, free or quasi-free type.

4.4.5 Example: D_4

We now consider, as an example, the case D_4. For any spin assignment in the D_4 model, the spin states on one sublattice are all 2, while each spin state on the other is 1, 3 or 4, so that the model can be regarded as a three-state model on the latter sublattice. The bulk weights of this model can be shown to be those of the critical three-state Potts model. These bulk weights are also invariant under any $\mathcal{S}_3$ permutation of the Potts spin states. We shall therefore use the more natural labelling of the nodes of D_4, $1 \mapsto A$, $2 \mapsto 0$, $3^+ \mapsto B$ and $3^- \mapsto C$; that is,

$D_4 \;=$ 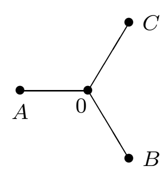

. (4.59)

The D_4 fused adjacency matrices are, from (4.12),

$$F^1 = F^5 = \begin{pmatrix} 1 & 0 & 0 & 0 \\ 0 & 1 & 0 & 0 \\ 0 & 0 & 1 & 0 \\ 0 & 0 & 0 & 1 \end{pmatrix} \qquad F^2 = F^4 = \begin{pmatrix} 0 & 1 & 0 & 0 \\ 1 & 0 & 1 & 1 \\ 0 & 1 & 0 & 0 \\ 0 & 1 & 0 & 0 \end{pmatrix}$$
$$F^3 = \begin{pmatrix} 0 & 0 & 1 & 1 \\ 0 & 2 & 0 & 0 \\ 1 & 0 & 0 & 1 \\ 1 & 0 & 1 & 0 \end{pmatrix} \qquad F^5 = \begin{pmatrix} 0 & 0 & 0 & 0 \\ 0 & 0 & 0 & 0 \\ 0 & 0 & 0 & 0 \\ 0 & 0 & 0 & 0 \end{pmatrix}, \tag{4.60}$$

where the rows and columns are ordered A, 0, B, C. Using these and (4.56), we find that the D_4 boundary edge weights are, up to normalisation and a simple gauge transformation on the $(2,0)$ and $(3,0)$ boundary conditions which makes their $\mathcal{S}_3$ symmetry properties more apparent, as given in Table 3.

C	$E(C,0)_{11} = 1$	$E(0,A)_{11} =$ $E(0,B)_{11} = 1$	$E(A,0)_{11} =$ $E(B,0)_{11} = 1$	$E(0,C)_{11} = 1$
B	$E(B,0)_{11} = 1$	$E(0,A)_{11} =$ $E(0,C)_{11} = 1$	$E(A,0)_{11} =$ $E(C,0)_{11} = 1$	$E(0,B)_{11} = 1$
0	$E(0,A)_{11} =$ $E(0,B)_{11} =$ $E(0,C)_{11} = 1$	$E(A,0)_{11} = 1$ $E(A,0)_{12} = 0$ $E(B,0)_{11} = -1/2$ $E(B,0)_{12} = \sqrt{3}/2$ $E(C,0)_{11} = -1/2$ $E(C,0)_{12} = -\sqrt{3}/2$	$E(0,A)_{11} = 1$ $E(0,A)_{12} = 0$ $E(0,B)_{11} = -1/2$ $E(0,B)_{12} = \sqrt{3}/2$ $E(0,C)_{11} = -1/2$ $E(0,C)_{12} = -\sqrt{3}/2$	$E(A,0)_{11} =$ $E(B,0)_{11} =$ $E(C,0)_{11} = 1$
A	$E(A,0)_{11} = 1$	$E(0,B)_{11} =$ $E(0,C)_{11} = 1$	$E(B,0)_{11} =$ $E(C,0)_{11} = 1$	$E(0,A)_{11} = 1$
a / r	1	2	3	4

Table 3: D_4 boundary edge weights

We see that the eight D_4 boundary conditions at the conformal point are:

- $(1, A) \leftrightarrow (4, A) \leftrightarrow$ A fixed
- $(1, B) \leftrightarrow (4, B) \leftrightarrow$ B fixed
- $(1, C) \leftrightarrow (4, C) \leftrightarrow$ C fixed
- $(2, A) \leftrightarrow (3, A) \leftrightarrow$ B and C mixed with equal weight
- $(2, B) \leftrightarrow (3, B) \leftrightarrow$ A and C mixed with equal weight
- $(2, C) \leftrightarrow (3, C) \leftrightarrow$ A and B mixed with equal weight
- $(1, 0) \leftrightarrow (4, 0) \leftrightarrow$ free
- $(2, 0) \leftrightarrow (3, 0) \leftrightarrow$ quasi-free in which same-spin pairs have weight 1 and different-spin pairs have weight $-1/2$

The nature of the last boundary condition is best seen by considering the $(2, 0)$ boundary weights at the conformal point, these being, up to normalisation,

$$B^{2,0}\left(0 \begin{array}{cc} d & 1 \\ b & 1 \end{array} \middle| \xi, \xi\right) = \begin{cases} 1\,; & b = d \\ -1/2\,; & b \neq d\,, \end{cases} \qquad b, d \in \{A, B, C\}\,. \tag{4.61}$$

This is therefore a boundary condition on nearest-neighbour pairs of Potts spins, in which like and unlike neighbours are associated with weights 1 and $-1/2$ respectively.

We see that the last two D_4 boundary conditions are $\mathcal{S}_3$ symmetric, while the first six are not. In fact, the $(2, 0)$ boundary weights (4.61) represent the only possibility, other than reproducing the $(1, 0) \leftrightarrow (4, 0)$ weights, which is $\mathcal{S}_3$ symmetric and consistent with a decomposition (3.48) in which γ is summed over two values.

4.4.6 E Graphs

For the E graphs, there are a large number of boundary conditions at the conformal point (specifically, 30 for E_6, 56 for E_7 and 112 for E_8) and many of these are in turn associated with a large number of boundary edge weights. Therefore, since it is straightforward and more practical to obtain the numerical values for these weights using a computer, we do not list them here. However, as an example, we do give the sets of E_6 boundary edges.

The E_6 fused adjacency matrices are

$$F^1=\begin{pmatrix}1&0&0&0&0&0\\0&1&0&0&0&0\\0&0&1&0&0&0\\0&0&0&1&0&0\\0&0&0&0&1&0\\0&0&0&0&0&1\end{pmatrix}\quad F^2=\begin{pmatrix}0&1&0&0&0&0\\1&0&1&0&0&0\\0&1&0&1&0&1\\0&0&1&0&1&0\\0&0&0&1&0&0\\0&0&1&0&0&0\end{pmatrix}\quad F^3=\begin{pmatrix}0&0&1&0&0&0\\0&1&0&1&0&1\\1&0&2&0&1&0\\0&1&0&1&0&1\\0&0&1&0&0&0\\0&1&0&1&0&0\end{pmatrix}$$

$$F^4=\begin{pmatrix}0&0&0&1&0&1\\0&0&2&0&1&0\\0&2&0&2&0&1\\1&0&2&0&0&0\\0&1&0&0&0&1\\1&0&1&0&1&0\end{pmatrix}\quad F^5=\begin{pmatrix}0&0&1&0&1&0\\0&1&0&2&0&1\\1&0&3&0&1&0\\0&2&0&1&0&1\\1&0&1&0&0&0\\0&1&0&1&0&1\end{pmatrix}\quad F^6=\begin{pmatrix}0&1&0&1&0&0\\1&0&2&0&1&0\\0&2&0&2&0&2\\1&0&2&0&1&0\\0&1&0&1&0&0\\0&0&2&0&0&0\end{pmatrix}$$

$$F^7=\begin{pmatrix}1&0&1&0&0&0\\0&2&0&1&0&1\\1&0&3&0&1&0\\0&1&0&2&0&1\\0&0&1&0&1&0\\0&1&0&1&0&1\end{pmatrix}\quad F^8=\begin{pmatrix}0&1&0&0&0&1\\1&0&2&0&0&0\\0&2&0&2&0&1\\0&0&2&0&1&0\\0&0&0&1&0&1\\1&0&1&0&1&0\end{pmatrix}\quad F^9=\begin{pmatrix}0&0&1&0&0&0\\0&1&0&1&0&1\\1&0&2&0&1&0\\0&1&0&1&0&1\\0&0&1&0&0&0\\0&1&0&1&0&0\end{pmatrix}\tag{4.62}$$

$$F^{10}=\begin{pmatrix}0&0&0&1&0&0\\0&0&1&0&1&0\\0&1&0&1&0&1\\1&0&1&0&0&0\\0&1&0&0&0&0\\0&0&1&0&0&0\end{pmatrix}\quad F^{11}=\begin{pmatrix}0&0&0&0&1&0\\0&0&0&1&0&0\\0&0&1&0&0&0\\0&1&0&0&0&0\\1&0&0&0&0&0\\0&0&0&0&0&1\end{pmatrix}\quad F^{12}=\begin{pmatrix}0&0&0&0&0&0\\0&0&0&0&0&0\\0&0&0&0&0&0\\0&0&0&0&0&0\\0&0&0&0&0&0\\0&0&0&0&0&0\end{pmatrix}.$$

Using these, we find that the E_6 boundary edges are as given in Table 4. In this table we also give, for each $(b,c)\in\mathcal{E}^{ra}$, the values of F^r_{ba} and F^{r+1}_{ca} as successive superscripts.

6	$(6,3)^{11}$	$(3,2)^{11}$ $(3,4)^{11}$	$(2,1)^{11}$ $(2,3)^{11}$ $(4,3)^{11}$ $(4,5)^{11}$	$(1,2)^{11}$ $(3,2)^{11}$ $(3,4)^{11}$ $(3,6)^{11}$ $(5,4)^{11}$	$(2,3)^{12}$ $(4,3)^{12}$ $(6,3)^{12}$	$(3,2)^{21}$ $(3,4)^{21}$ $(3,6)^{21}$	$(2,1)^{11}$ $(2,3)^{11}$ $(4,3)^{11}$ $(4,5)^{11}$ $(6,3)^{11}$	$(1,2)^{11}$ $(3,2)^{11}$ $(3,4)^{11}$ $(5,4)^{11}$	$(2,3)^{11}$ $(4,3)^{11}$	$(3,6)^{11}$
5	$(5,4)^{11}$	$(4,3)^{11}$	$(3,2)^{11}$ $(3,6)^{11}$	$(2,1)^{11}$ $(2,3)^{11}$ $(6,3)^{11}$	$(1,2)^{11}$ $(3,2)^{11}$ $(3,4)^{11}$	$(2,3)^{11}$ $(4,3)^{11}$ $(4,5)^{11}$	$(3,4)^{11}$ $(3,6)^{11}$ $(5,4)^{11}$	$(4,3)^{11}$ $(6,3)^{11}$	$(3,2)^{11}$	$(2,1)^{11}$
4	$(4,3)^{11}$ $(4,5)^{11}$	$(3,2)^{11}$ $(3,4)^{11}$ $(3,6)^{11}$ $(5,4)^{11}$	$(2,1)^{11}$ $(2,3)^{12}$ $(4,3)^{12}$ $(6,3)^{12}$	$(1,2)^{12}$ $(3,2)^{22}$ $(3,4)^{21}$ $(3,6)^{21}$	$(2,1)^{21}$ $(2,3)^{22}$ $(4,3)^{12}$ $(4,5)^{11}$ $(6,3)^{12}$	$(1,2)^{11}$ $(3,2)^{21}$ $(3,4)^{22}$ $(3,6)^{21}$ $(5,4)^{12}$	$(2,3)^{12}$ $(4,3)^{22}$ $(4,5)^{21}$ $(6,3)^{12}$	$(3,2)^{21}$ $(3,4)^{21}$ $(3,6)^{21}$ $(5,4)^{11}$	$(2,1)^{11}$ $(2,3)^{11}$ $(4,3)^{11}$ $(6,3)^{11}$	$(1,2)^{11}$ $(3,2)^{11}$
3	$(3,2)^{11}$ $(3,4)^{11}$ $(3,6)^{11}$	$(2,1)^{11}$ $(2,3)^{12}$ $(4,3)^{12}$ $(4,5)^{11}$ $(6,3)^{12}$	$(1,2)^{12}$ $(3,2)^{22}$ $(3,4)^{22}$ $(3,6)^{21}$ $(5,4)^{12}$	$(2,1)^{21}$ $(2,3)^{23}$ $(4,3)^{23}$ $(4,5)^{21}$ $(6,3)^{13}$	$(1,2)^{12}$ $(3,2)^{32}$ $(3,4)^{32}$ $(3,6)^{32}$ $(5,4)^{12}$	$(2,1)^{21}$ $(2,3)^{23}$ $(4,3)^{23}$ $(4,5)^{21}$ $(6,3)^{23}$	$(1,2)^{12}$ $(3,2)^{32}$ $(3,4)^{32}$ $(3,6)^{31}$ $(5,4)^{12}$	$(2,1)^{21}$ $(2,3)^{22}$ $(4,3)^{22}$ $(4,5)^{21}$ $(6,3)^{12}$	$(1,2)^{11}$ $(3,2)^{21}$ $(3,4)^{21}$ $(3,6)^{21}$ $(5,4)^{11}$	$(2,3)^{11}$ $(4,3)^{11}$ $(6,3)^{11}$
2	$(2,1)^{11}$ $(2,3)^{11}$	$(1,2)^{11}$ $(3,2)^{11}$ $(3,4)^{11}$ $(3,6)^{11}$	$(2,3)^{12}$ $(4,3)^{12}$ $(4,5)^{11}$ $(6,3)^{12}$	$(3,2)^{21}$ $(3,4)^{22}$ $(3,6)^{21}$ $(5,4)^{12}$	$(2,1)^{11}$ $(2,3)^{12}$ $(4,3)^{22}$ $(4,5)^{21}$ $(6,3)^{12}$	$(1,2)^{12}$ $(3,2)^{22}$ $(3,4)^{21}$ $(3,6)^{21}$ $(5,4)^{11}$	$(2,1)^{21}$ $(2,3)^{22}$ $(4,3)^{12}$ $(6,3)^{12}$	$(1,2)^{11}$ $(3,2)^{21}$ $(3,4)^{21}$ $(3,6)^{21}$	$(2,3)^{11}$ $(4,3)^{11}$ $(4,5)^{11}$ $(6,3)^{11}$	$(3,4)^{11}$ $(5,4)^{11}$
1	$(1,2)^{11}$	$(2,3)^{11}$	$(3,4)^{11}$ $(3,6)^{11}$	$(4,3)^{11}$ $(4,5)^{11}$ $(6,3)^{11}$	$(3,2)^{11}$ $(3,4)^{11}$ $(5,4)^{11}$	$(2,1)^{11}$ $(2,3)^{11}$ $(4,3)^{11}$	$(1,2)^{11}$ $(3,2)^{11}$ $(3,6)^{11}$	$(2,3)^{11}$ $(6,3)^{11}$	$(3,4)^{11}$	$(4,5)^{11}$
$a \backslash r$	1	2	3	4	5	6	7	8	9	10

Table 4: E_6 boundary edges

From this table, the properties (4.26) and (4.31) are immediately apparent, and we can also gain some understanding of the nature of each of the 30 boundary conditions at the conformal point.

4.5 Realisation of Conformal Boundary Conditions

We now consider the relationship between the integrable boundary conditions of the A–D–E lattice models and the conformal boundary conditions of the critical series of unitary minimal $\hat{s\ell}(2)$ conformal field theories.

Each conformal field theory of this type on a torus or cylinder is associated with two graphs, the A graph A_{g-2} and an A, D or E graph $\mathcal{G}$ with Coxeter number g, this theory being denoted $\mathcal{M}(A_{g-2},\mathcal{G})$. As shown in [14, 15, 16], the lattice model based on $\mathcal{G}$, with ψ the Perron-Frobenius eigenvector and $0<u<\lambda$, can be associated with the field theory $\mathcal{M}(A_{g-2},\mathcal{G})$.

In [7], it was found that the complete set of conformal boundary conditions of $\mathcal{M}(A_{g-2},\mathcal{G})$ on a cylinder is labelled by the set of pairs (r,a), with $r\in\{1,\ldots,g-2\}$, $a\in\mathcal{G}$ and (r,a) and $(g-r-1,\bar{a})$ being considered as equivalent. We immediately see that this classification is identical to that of the boundary conditions of the corresponding lattice model at the conformal point.

It was also shown in [7] that the partition function of $\mathcal{M}(A_{g-2},\mathcal{G})$ on a cylinder with conformal boundary conditions (r_1,a_1) and (r_2,a_2) is given by

$$Z_{r_1a_1|r_2a_2}(q) \;=\; \sum_{r=1}^{g-2}\sum_{s=1}^{g-1} F(A_{g-2})^r_{r_1r_2}\; F(\mathcal{G})^s_{a_1a_2}\;\chi_{(r,s)}(q)\,, \tag{4.63}$$

where q is the modular parameter, $F(A_{g-2})^r$ and $F(\mathcal{G})^s$ denote the fused adjacency matrices of A_{g-2} and $\mathcal{G}$, and $\chi_{(r,s)}$ is the character of the Verma module of the Virasoro algebra with central charge and highest weight

$$c \;=\; 1-\frac{6}{g\,(g-1)} \qquad \text{and} \qquad \Delta_{(r,s)} \;=\; \frac{(r\,g-s\,(g-1))^2-1}{4\,g\,(g-1)}\,. \tag{4.64}$$

The equivalence of the (r,a) and $(g-r-1,\bar{a})$ conformal boundary conditions is apparent by using (4.16) and the relation $\Delta_{(g-r-1,g-s)}=\Delta_{(r,s)}$ to observe that the partition function (4.63) is unchanged by applying this transformation to either of the boundary condition labels.

We now assert that, in the continuum scaling limit, the (r,a) boundary condition in the lattice model at the conformal and isotropic point provides a realisation of the (r,a) conformal boundary condition of the corresponding field theory. In particular, we expect that, as $N\to\infty$, the eigenvalues of $\boldsymbol{D}^N_{r_1a_1|r_2a_2}(\lambda/2,\lambda/2,\lambda/2)$ can be arranged in towers, with each tower labelled by a pair (r,s) and the multiplicity of tower (r,s) given by $F(A_{g-2})^r_{r_1r_2}\;F(\mathcal{G})^s_{a_1a_2}$. We further expect that the j'th largest eigenvalue in this tower has the form

$$\Lambda^{(r,s)j}_{r_1a_1|r_2a_2} \;=\; \exp\Big[-2N\mathcal{F} \,-\, 2f_{r_1|r_2} \,+\, 2\pi(c/24-\Delta_{(r,s)}-k_{(r,s)j})/N \,+\, \mathrm{o}(1/N)\Big], \quad (4.65)$$

where $\mathcal{F}$ is the bulk free energy per lattice face, which depends only on g, $f_{r_1|r_2}$ is the boundary free energy per lattice row, which depends only on g, r_1 and r_2, c and $\Delta_{(r,s)}$ are as given in (4.64), and $k_{(r,s)j}$ are nonnegative integers given through the expansion of the Virasoro characters by

$$\chi_{(r,s)}(q) \;=\; q^{-c/24+\Delta_{(r,s)}}\sum_{j=1}^{\infty} q^{k_{(r,s)j}}\,, \quad k_{(r,s)j}\le k_{(r,s)j+1}\,. \quad (4.66)$$

With the eigenvalues appearing in this tower structure, it follows using (3.57) that, as $N\to\infty$, the lattice model and conformal partition functions are related by

$$\begin{aligned}&\boldsymbol{Z}^{NM}_{r_1a_1|r_2a_2}(\lambda/2,\lambda/2,\lambda/2) \;\sim\\ &\qquad \exp(-2MN\mathcal{F}-2Mf_{r_1|r_2})\;Z_{r_1a_1|r_2a_2}(q)\,, \quad q=\exp(-2\pi M/N)\,.\end{aligned} \quad (4.67)$$

We note that we also expect related conformal behaviour in a lattice model which is at the conformal point and has $0<u<\lambda$, but which is no longer at the isotropic point $u=\lambda/2$.

The expectation that the lattice model boundary conditions correspond in this way to the conformal boundary conditions is supported by the results of numerical studies we have performed, the matching of the identifications made here of the nature of the lattice realisations of certain conformal boundary conditions with those made in other studies, the consistency of all of the symmetry properties of the lattice model partition function with those of the conformal partition function, and analytic confirmation in several cases.

In our numerical studies, we evaluated the eigenvalues of $\boldsymbol{D}^N_{r_11|r_2s}(\lambda/2,\lambda/2,\lambda/2)$ for certain A graphs, selected values of r_1, r_2 and s, and several successive values of

N. We then extrapolated these results to large N and verified consistency with (4.65) for these cases. This numerical data, used with (4.44), also implied consistency with (4.65) for all of the related A, D and E cases.

Regarding the identification of the nature of the lattice realisations of particular conformal boundary conditions, this was done for all A_3 cases and all D_4 cases except $(2,0)$ in [1, 17], for all $(1,a)$ and $(r,1)$ cases of A_{g-1} and $D_{\frac{g}{2}+1}$ in [18], for all A_4 cases in [23], and for the $(2,0)$ case of D_4 in [27]. In all of these studies, the lattice model boundary conditions were shown to have exactly the same basic features as those found here.

Proceeding to the consistency of symmetry properties, it follows straightforwardly from (4.63) and the properties of the fused adjacency matrices that the $\mathcal{M}(A_{g-2},\mathcal{G})$ partition function satisfies

$$\begin{aligned}
Z_{r_1a_1|r_2a_2}(q) \;&=\; Z_{r_2a_2|r_1a_1}(q) \;=\; Z_{r_2a_1|r_1a_2}(q)\\
&=\; Z_{r_1\bar{a}_1|r_2\bar{a}_2}(q) \;=\; Z_{g-r_1-1,\bar{a}_1|g-r_2-1,\bar{a}_2}(q)\\
\sum_{a_1',a_2'\in\mathcal{G}} F(\mathcal{G})^{r_1}_{a_1a_1'}\,F(\mathcal{G})^{r_2}_{a_2a_2'}\,Z_{r_1'a_1'|r_2'a_2'}(q) \;&=\; \\
&\sum_{a_1',a_2'\in\mathcal{G}} F(\mathcal{G})^{r_2}_{a_1a_1'}\,F(\mathcal{G})^{r_1}_{a_2a_2'}\,Z_{r_1'a_1'|r_2'a_2'}(q)\\
\sum_{a\in\mathcal{G}} F(\mathcal{G})^{s'}_{a_1a}\,Z_{r_1a|r_2a_2}(q) \;&=\; \sum_{s=1}^{g-1} F(\mathcal{G})^{s'}_{a_1a_2}\,Z_{r_1s'|r_2s}(q)\,.
\end{aligned} \tag{4.68}$$

We immediately see that these equalities are consistent with the lattice relations (3.66), (3.68), (4.29), (4.38), (3.72) and (4.41) respectively. We also note that certain cases of the last equality of (4.68) and its lattice version (4.41), mostly with $s'=r_1=r_2=1$, were considered numerically and analytically in [1, 18, 19, 20, 21, 22], while in [26] free combinations of $(1,a)$ lattice boundary conditions in A_{g-1} were studied analytically leading to (4.45) with $r_1=r_2=1$ and a sum on a_1 and a_2. However, in all of these studies, the orientation of the lattice differed from that used here by a rotation of 45 degrees.

Finally, the partition function relation (4.67) has been proved analytically using techniques based on the Yang-Baxter and boundary Yang-Baxter equations for a lattice with the same orientation as that used here for all A_3 cases in [24] and for all A_4 cases which lead to a single character on the right side of (4.63) in [25].

5 . Discussion

We have presented various results on integrable boundary conditions for the A–D–E lattice models. In particular, we have explicitly constructed boundary weights, derived general symmetry properties and studied the relationship with conformal boundary conditions.

The formalism presented here can be generalised in several natural ways, each of which enables the consideration of other integrable lattice models and associated rational conformal field theories. We expect that the corresponding integrable boundary conditions provide realisations of the conformal boundary conditions of these field theories, although we acknowledge that for many of these models only the bulk weights are currently known and that explicitly obtaining boundary weights may involve certain technical challenges. Nevertheless, in conclusion, we list these other cases and indicate their connections with those studied here:

• By choosing in (3.4) an eigenvector of an A–D–E adjacency matrix other than the Perron-Frobenius eigenvector, lattice models are obtained which correspond to the $\mathcal{M}(A_{h-1},\mathcal{G})$ nonunitary minimal theories with $h<g-1$. In fact, this also includes all of the $\mathcal{M}(A_{h-1},A_{g-1})$ theories with $g<h-1$, since in this case g and h are interchangeable.

• By taking $\mathcal{G}$ as the Dynkin diagram of an affine A, D or E Lie algebra, lattice models are obtained which correspond to certain conformal field theories with central charge $c=1$. We note that in these cases the Perron-Frobenius eigenvalue is 2 so that, from (3.4), s is given by the second case of (2.2) and, from (2.11), there are infinitely many fusion levels.

• By replacing the relations of (2.1) with those of the Hecke algebra, certain lattice models and conformal field theories associated with $\hat{s\ell}(n)$, for $n>2$, can be obtained. In this case, although the lattice models become significantly different, we expect that most of the results of Section 2 remain unchanged

• By using the dilute Temperley-Lieb algebra instead of the Temperley-Lieb algebra, lattice models which correspond to the so-called tricritical series of unitary minimal theories, $\mathcal{M}(A_g, \mathcal{G})$, can be obtained. However, we note that the dilute Temperley-Lieb algebra contains considerably more generators than the Temperley-Lieb algebra, so that the formalism would be more complicated from the outset.

• It is also apparent that lattice models whose bulk weights are given by fused square blocks of A–D–E bulk weights could be considered by applying some relatively straightforward extensions to the formalism. The field theories associated with these models include certain superconformal theories. The cases of the A models involving only diagonal boundary weights were studied in [31], where it was shown that the double-row transfer matrices of the standard and fused model together satisfy a hierarchy of functional equations. We expect that equations of a similar form can be derived, using the boundary inversion relation (3.41) and other local properties, for the remaining A–D–E cases, such equations being important in the analytic determination of transfer matrix eigenvalues.

• Finally, we mention the off-critical A and D models, which can be associated with perturbed conformal field theories. The bulk weights in these cases can no longer be expressed in terms of the Temperley-Lieb algebra, but a fusion procedure still exists and boundary weights constructed from fused blocks of bulk weights still satisfy the boundary Yang-Baxter equation. Some integrable boundary weights are known for these cases, as listed in [32], and it is expected that each of the A and D boundary conditions found here corresponds to the critical limit of an off-critical integrable boundary condition.

Acknowledgements

PAP is supported by the Australian Research Council. We are thankful to Jean-Bernard Zuber for useful discussions and for his hospitality at CEA-Saclay, where some of this work was done.

References

[1] J. L. Cardy *Nucl. Phys. B* **324** (1989) 581–596 *Boundary Conditions, Fusion Rules and the Verlinde Formula*

[2] E. K. Sklyanin *J. Phys. A* **21** (1988) 2375–2389 *Boundary Conditions for Integrable Quantum Systems*

[3] R. J. Baxter *Exactly Solved Models in Statistical Mechanics* (Academic Press, 1982)

[4] R. E. Behrend and P. A. Pearce *J. Phys. A* **29** (1996) 7827–7835 *A Construction of Solutions to Reflection Equations for Interaction-Round-a-Face Models*

[5] R. E. Behrend, P. A. Pearce and J.-B. Zuber *J. Phys. A* **31** (1998) L763–L770 *Integrable Boundaries, Conformal Boundary Conditions and A–D–E Fusion Rules*

[6] R. E. Behrend, P. A. Pearce, V. B. Petkova and J.-B. Zuber *Phys. Lett. B* **444** (1998) 163–166 *On the Classification of Bulk and Boundary Conformal Field Theories*

[7] R. E. Behrend, P. A. Pearce, V. B. Petkova and J.-B. Zuber hep-th/9908036 *Boundary Conditions in Rational Conformal Field Theories* To appear in *Nucl. Phys. B*

[8] V. Pasquier *Nucl. Phys. B* **285** (1987) 162–172 *Two-Dimensional Critical Systems Labelled by Dynkin Diagrams*

[9] A. A. Belavin, A. M. Polyakov and A. B. Zamolodchikov *Nucl. Phys. B* **241** (1984) 333–380 *Infinite Conformal Symmetry in Two-Dimensional Quantum Field Theory*

[10] D. Friedan, Z. Qiu and S. Shenker *Phys. Rev. Lett.* **52** (1984) 1575–1578 *Conformal Invariance, Unitarity and Critical Exponents in Two Dimensions*

[11] A. Cappelli, C. Itzykson, and J.-B. Zuber *Nucl. Phys. B* **280** (1987) 445–465 *Modular Invariant Partition Functions in Two Dimensions*

[12] A. Cappelli, C. Itzykson, and J.-B. Zuber *Comm. Math. Phys.* **113** (1987) 1–26 *The A–D–E Classification of Minimal and* $A_1^{(1)}$ *Conformal Invariant Theories*

[13] A. Kato *Mod. Phys. Lett. A* **2** (1987) 585–600 *Classification of Modular Invariant Partition Functions in Two Dimensions*

[14] D. A. Huse *Phys. Rev. B* **30** (1984) 3908–3915 *Exact Exponents for Infinitely Many New Multicritical Points*

[15] V. Pasquier *J. Phys. A* **20** (1987) 5707–5717 *Operator Content of the A–D–E Lattice Models*

[16] V. Pasquier *J. Phys. A* **20** (1987) L1229–L1237 *Lattice Derivation of Modular Invariant Partition Functions on the Torus*

[17] J. L. Cardy *Nucl. Phys. B* **275** (1986) 200–218 *Effect of Boundary Conditions on the Operator Content of Two-Dimensional Conformally Invariant Theories*

[18] H. Saleur and M. Bauer *Nucl. Phys. B* **320** (1989) 591–624 *On Some Relations Between Local Height Probabilities and Conformal Invariance*

[19] P. Di Francesco and J.-B. Zuber *$SU(N)$ Lattice Integrable Models and Modular Invariance* in S. Randjbar-Daemi, E. Sezgin and J.-B. Zuber (Eds.) *Recent Developments in Conformal Field Theories* (World Scientific, 1990) 179–215

[20] V. Pasquier and H. Saleur *Nucl. Phys. B* **330** (1990) 523–556 *Common Structures Between Finite Systems and Conformal Field Theories Through Quantum Groups*

[21] P. Di Francesco *Int. J. Mod. Phys. A* **7** (1992) 407–500 *Integrable Lattice Models, Graphs and Modular Invariant Conformal Field Theories*

[22] P. Dorey *Int. J. Mod. Phys. A* **8** (1993) 193–208 *Partition Functions, Intertwiners and the Coxeter Element*

[23] L. Chim *Int. J. Mod. Phys. A* **11** (1996) 4491–4512 *Boundary S-Matrix for the Tricritical Ising Model*

[24] D. L. O'Brien, P. A. Pearce and S. O. Warnaar *Physica A* **228** (1996) 63–77 *Finitized Conformal Spectrum of the Ising Model on the Cylinder and Torus*

[25] D. L. O'Brien, P. A. Pearce and S. O. Warnaar *Nucl. Phys. B* **501** (1997) 773–799 *Analytic Calculation of Conformal Partition Functions: Tricritical Hard Squares with Fixed Boundaries*

[26] M. T. Batchelor *Physica A* **251** (1998) 132–142 *Surface Operator Content of the A_L Face Models*

[27] I. Affleck, M. Oshikawa and H. Saleur *J. Phys. A* **31** (1998) 5827–5842 *Boundary Critical Phenomena in the Three-State Potts Model*

[28] A. L. Owczarek and R. J. Baxter *J. Stat. Phys.* **49** (1987) 1093–1115 *A Class of Interaction-Round-a-Face Models and its Equivalence with an Ice-Type Model*

[29] H. Fan, B. Y. Hou and K. J. Shi *J. Phys. A* **28** (1995) 4743–4749 *General Solution of Reflection Equation for Eight-Vertex SOS Model*

[30] C. Ahn and W. M. Koo *Nucl. Phys. B* **468** (1996) 461–486 *Boundary Yang-Baxter Equation in the RSOS/SOS Representation*

[31] R. E. Behrend, P. A. Pearce and D. L. O'Brien *J. Stat. Phys.* **84** (1996) 1–48 *Interaction-Round-a-Face Models with Fixed Boundary Conditions: The ABF Fusion Hierarchy*

[32] R. E. Behrend and P. A. Pearce *Int. J. Mod. Phys. B* **11** (1997) 2833–2847 *Boundary Weights for Temperley-Lieb and Dilute Temperley-Lieb Models*

[33] C. Ahn and C. K. You *J. Phys. A* **31** (1998) 2109–2121 *Complete Non-diagonal Reflection Matrices of RSOS/SOS and Hard Hexagon Models*

[34] H. N. V. Temperley and E. H. Lieb *Proc. Roy. Soc. Lond. A* **322** (1971) 251–280 *Relations Between the 'Percolation' and 'Colouring' Problem and Other Graph-Theoretical Problems Associated with Regular Planar Lattices: Some Exact Results for the 'Percolation' Problem*

[35] T. Deguchi, Y. Akutsu and M. Wadati *J. Phys. Soc. Japan* **57** (1988) 757–776 *Exactly Solvable Models and New Link Polynomials. III. Two-Variable Topological Invariants*

[36] T. Deguchi, M. Wadati and Y. Akutsu *J. Phys. Soc. Japan* **57** (1988) 1905–1923 *Exactly Solvable Models and New Link Polynomials. V. Yang-Baxter Operator and Braid-Monoid Algebra*

[37] M. Wadati, T. Deguchi and Y. Akutsu *Phys. Rep.* **180** (1989) 247–332 *Exactly Solvable Models and Knot Theory*

[38] P. P. Kulish, N. Y. Reshetikhin and E. K. Sklyanin *Lett. Math. Phys.* **5** (1981) 393–403 *Yang-Baxter Equation and Representation Theory: I*

[39] E. Date, M. Jimbo, T. Miwa and M. Okado *Lett. Math. Phys.* **12** (1986) 209–215 *Fusion of the Eight Vertex SOS Model*

[40] E. Date, M. Jimbo, T. Miwa and M. Okado *Lett. Math. Phys.* **14** (1987) 97 *Erratum and Addendum: Fusion of the Eight Vertex SOS Model*

[41] E. Date, M. Jimbo, A. Kuniba, T. Miwa and M. Okado *Adv. Stud. Pure Math.* **16** (1988) 17–122 *Exactly Solvable SOS Models II: Proof of the Star-Triangle Relation and Combinatorial Identities*

[42] Y. K. Zhou and P. A. Pearce *Int. J. Mod. Phys. B* **8** (1994) 3531–3577 *Fusion of A–D–E Lattice Models*

[43] P. P. Kulish *Yang-Baxter Equation and Reflection Equations in Integrable Models* in H. Grosse and L. Pittner (Eds.) *Low-Dimensional Models in Statistical Physics and Quantum Field Theory* (Springer-Verlag, 1996) 125–144

[44] I. V. Cherednik *Teor. Mat. Fiz.* **61** (1984) 35–44 *Factorizing Particles on a Half Line and Root Systems*

[45] G. E. Andrews, R. J. Baxter and P. J. Forrester *J. Stat. Phys.* **35** (1984) 193–266 *Eight-Vertex SOS Model and Generalized Rogers-Ramanujan-Type Identities*

[46] V. Pasquier *J. Phys. A* **20** (1987) L217–L220 *Exact Solubility of the D_n Series*

[47] P. Di Francesco and J.-B. Zuber *Nucl. Phys. B* **338** (1990) 602–646 *$SU(N)$ Lattice Integrable Models Associated with Graphs*

[48] P. Roche *Comm. Math. Phys.* **127** (1990) 395–424 *Ocneanu Cell Calculus and Integrable Lattice Models*

[49] P. A. Pearce and Y. K. Zhou *Int. J. Mod. Phys. B* **7** (1993) 3649–3705 *Intertwiners and A–D–E Lattice Models*